

The influence of normal-, bending-
and shear stresses on the ultimate
compression force exerted laterally
to European rolled sections.

Report 6-80-5

February 1980

ir. P. Zoetemeijer.

Delft University of Technology
Department of Civil Engineering
Stevin laboratory: Steel structures

Delft University of Technology
Faculty of Civil Engineering
Section Steelstructures
Stevin Laboratory
Stevinweg 11
2628 CN Delft
The Netherlands

Report 6-80-5

The influence of normal-, bending-
and shear stresses on the ultimate
compression force exerted laterally
to European rolled sections.

February 1980

ir. P. Zoetemeijer.

Contents	Page
0. Summary	1
1. Introduction	2
2. Test set-up	4
3. Test results	5
4. Discussion	9
5. Conclusions	13
6. Literature	14
Compilation of test results	15
Figures:	24

0. Summary

This report contains the results of tests carried out on European rolled sections.

The sections were loaded by lateral forces while axial bending and shear stresses were caused by other forces.

A comparison of the results has lead to decisions when the ultimate limit load of the lateral force has to be reduced and in what way.

1 Introduction

In [1] "Design rules for unstiffened welded connections" have been discussed.

To calculate the moment capacity of a beam-to-column connection, the moment at the end of the beam is replaced by a pair of statically equivalent forces in the flanges of the beam. A connection will reach its moment capacity when one or both of the following regions in the connection becomes critical:

a. The compression zone

a1. Buckling, crippling or yielding of the web of the column.

b. The tension zone

b1. yielding of the flange of the column

b2. yielding of the web of the column

Formulae have been given which allow to calculate the ultimate limit state loads for the two regions. However on the web panel of the column a plane stress situation exists and there is an interaction between normal stresses and shearing stresses following the von Mises yield criterion.

$$\sigma_c = \sqrt{\sigma_x^2 + \sigma_y^2 - \sigma_x \sigma_y + 3 \tau^2} \leq \sigma_y \quad (1)$$

That is the reason why for T- and Kneecconnections the ultimate limit load of the compression force was decreased according to this formula.

In this kind of connections the shearing force is equivalent to the tension and compression force. The limit state of the compression force was decreased too in connections with beams on either side of the column if the height of the beam or the load is asymmetric.

After research on bolted beam-to-column connections the question arose whether this decrease of the ultimate limit state is necessary or not. The von Mises yield criterion gives only information about the local stress situation.

A redistribution of stresses over the cross section of the column seems possible.

Tests were carried out to confirm this idea. This report deals with those tests.

A conclusion that interaction of the shearing and compression force is negligible, would imply that the limit state of a connection can be calculated by considering three separated regions.

- 1^o The tension side
- 2^o The compression side
- 3^o The shear zone

This would simplify the calculation considerably.

Tests with axial forces and bending moments in the section itself and loaded with lateral forces, have also been executed, to confirm knowledge already present.

This report is a translation of:

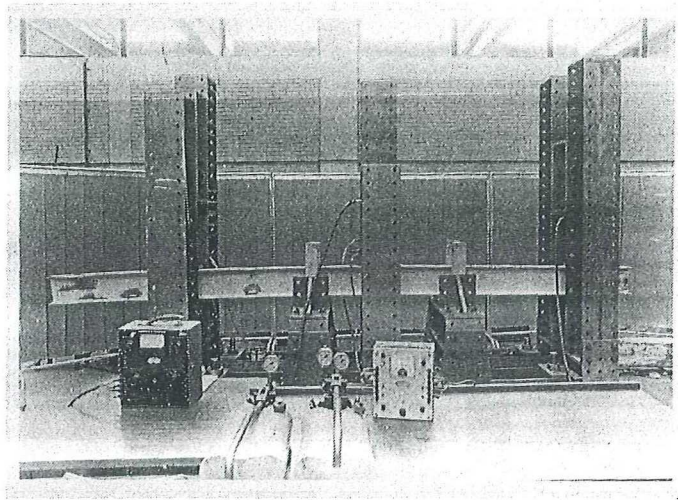
Report Stevin lab TH Delft no. 6-75-18, 1975

"Influence of normal-, bending- and shearing stresses on the ultimate compression force exerted laterally to European rolled sections", but contains some more results than the Dutch version.

2. Test set-up and measurements

The specimens were loaded as shown in the load-deformation diagrams.

A photograph of the test set-up is depicted in figure 2.1.



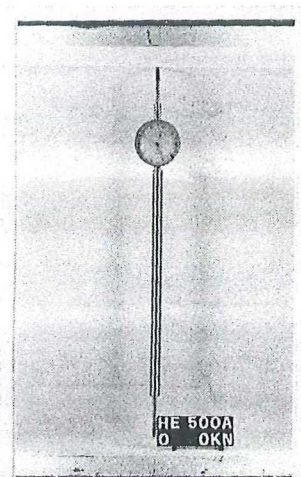
Test set-up

Figure 2.1.

Two jacks between two removable rigs gave the possibility to load the white beam in every desired way. In order to avoid lateral buckling the beam was sideways supported.

The beam was lime-washed to indicate great deformations by crumbling of the lime due to local yielding of the web. The loads were measured with loadcells.

The deformations were measured as shown in the photograph in figure 2.2.



The deformation of the web was measured between the flanges with dial gauges.

Figure 2.2.

3. Test results

The actual collapse loads of all specimens have been compiled; see the pages 15 to 22.

The following data have been given:

- the actual yield strength of the material
- photograph of the collapsed specimen
- test set up
- bending moment diagram
- shearing force diagram
- calculated bending stress
- calculated shearing stress
- stress due to an axial compressive force, if present.

The shearing stress was calculated with the formula:

$$\tau = \frac{D}{t_w (h - 2t_f)} \quad (2)$$

where:

D = shearing force

τ = shearing stress

t_f = thickness of the flange of a section

t_w = thickness of the web of a section

h = depth of a section

The shearing stress has been stated between brackets if a shear stiffener was present.

The stated bending stress was calculated at the transition from the flange to the web.

To be able to compare the results, several load deformation diagrams have been drawn in one figure, see the pages 24 to 36. To simplify the comparison, the deformation of the specimens with lateral loads on either side of the beam have been halved, because all deformations were measured over the complete height.

The following distinction has been made in the test results.

3.1. The influence of the length of the loading strip.

Diagrams in figure 3.1.1.

3.2. The influence of the shearing force caused by the lateral force itself, subdivided in:

- Results of specimens with- and without shear stiffeners

Diagrams in figure 3.2.1.

- Results of specimens with high shearing stresses and low bending stresses.

Diagrams in figure 3.2.2., 3.2.3. and 3.2.4.

- Results of specimens with high shearing stresses but no bending.

Diagrams in figure 3.2.5.

3.3. The influence of the bending stress, subdivided in:

- Results of specimens with high and low bending stresses and low shearing stresses.

Diagrams in figure 3.3.1. and 3.3.2.

- Results of specimens with high and low bending stresses and low- or no shearing stresses.

Diagrams in figure 3.3.3.

3.4. The influence of shearing stress already present in the section before loading.

Diagrams in figure 3.4.1.

3.5. The influence of tensile stress caused by bending already present before loading.

Diagrams in figure 3.5.1.

3.6. Results of specimens collapsed over the support.

Diagrams in figure 3.6.1.

3.7. The influence of axial compression force already present before loading.

Diagrams in figure 3.7.1.

The loading strips were not fastened to the sections. This differs from tests on welded beam-to-column connections where the flange of the beam was welded to the column flange.

Despite this, the same formula has been used as obtained from these tests [1], to calculate the limit state load of the lateral compression force.

$$\hat{F} = \sigma_e t_{wC} \{ t_{fb} + 5(r_C + t_{fC}) \} \quad (3)$$

where: σ_e = design value of the yield strength, here taken

$$\sigma_e = 240 \text{ N/mm}^2$$

t_{wC} = the thickness of the web of a column

t_{fb} = the thickness of the flange of the beam.

Here this value is the width of the loading-strip
(40 mm)

r_C = radius of the section

t_{fC} = the thickness of the flange of a column

The calculated limit state load has been depicted in the load deformation diagrams with the indication, " F_i ", where, "i" indicates the test number.

The actual yield stress was sometimes considerably higher than the design value.

Nevertheless the design value has been used, because the considered limit state is highly influenced by the instability phenomenon.

Other tests [1] had already shown that the collapse load is considerably influenced by normal stresses of more than 100 N/mm² present in the section.

That is the reason why the limit state loads of the specimens where compression or bending stresses were present, have been calculated with the formula.

$$\hat{F} = \sigma_e t_{wC} \{ t_{fb} + 5(r_C + t_{fC}) \} * \left(1,25 - 0,5 \frac{|\sigma|}{\sigma_e} \right) \quad (4)$$

where: $1,25 - 0,5 \frac{|\sigma|}{\sigma_e} \leq 1$

$$\text{and } |\sigma| = \frac{|N|}{A} + \frac{|M|}{I} \cdot e$$

where: N = normal force in the section

M = bending moment in the section

A = cross-sectional area of the section

I = moment of inertia of the section

e = distance from the centre of the section to
the transition from web to flange

and the other parameters in accordance with formula (3).

The reduction part of formula (4) has been adopted from [2].

The specimens in which shearing stress was already present before loading with the lateral force, showed a considerably lower collapse load than the specimens without shearing stresses (figure 3.4.1.).

The limit state load of these specimens have been calculated with the formula:

$$\hat{F} = \sigma_e t_{wC} \{t_{fb} + 5(r_c + t_{fC})\} * \sqrt{1 - \frac{3\tau^2}{\sigma_e^2}} \quad (5)$$

τ = shearing stress already present before loading with the lateral force and the other parameters in accordance with formula (3).

4. Discussion

The same division as made in the chapter about the test results will be used here

4.1. Length of the loading strip

The influence of the length of the loading strip appeared to be negligible.

This could be expected because formula (3) which is experimentally verified does not contain a parameter depending on the length of the loading strip.

4.2. The influence of the shearing-force caused by the lateral force itself.

A comparison of the results of the test specimens with and without shear stiffeners, as made in figure 3.2.1., shows evidently that the shearing force does not influence the collapse load of a lateral compression force.

Only the deformation seems to be influenced, but it must be taken into account that the deformation of the beam with lateral loads on either side, have been halved.

The deformations of the beams with one load were measured over the complete height of the beam.

The results of the specimens reported in figure 3.2.2. give instantaneously the impression that shearing stress influenced the collapse load of the lateral force.

But these specimens collapsed when the web completely yielded due to the shearing force.

The results of the specimens reported in figure 3.2.3. give no rise to special attention, they only confirm the conclusion drawn from the previous figures.

Specimen A12 in figure 3.2.3. was supported by a strip welded on the flange to simulate the tension side of a welded beam to column connection. This way of support was suspected to influence the result.

It did not in this specimen, but it did in specimen B9 in figure 3.2.4.

An exact solution for this phenomenon was not thought of. There is only a slight difference between the load deformation diagrams of specimen B3 and B9 which becomes only apparently in the plastic region.

It has been assumed that the difference is merely caused by the bending stress, rather than by the shearing stress.

It becomes apparent from figure 3.2.5. that there is no or a slight difference if bending stresses have been levelled.

The conclusion can be drawn that shearing stresses caused by the lateral force itself have no influence on the collapse load of a lateral exerted force.

4.3. The influence of the bending stress

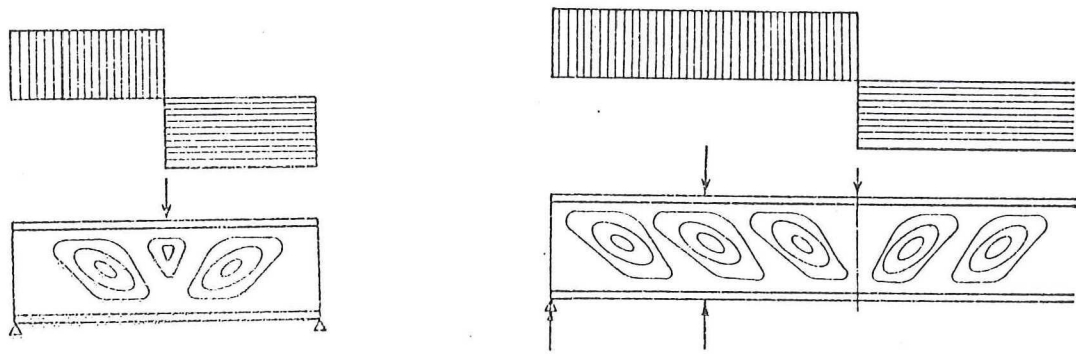
All results reported in figure 3.3.1. to figure 3.3.3. justify the conclusion that bending stresses influence the collapse load of a lateral force. This influence will be taken into account sufficiently by formula (4).

To simplify the calculation the bending stress in the very edge of the section can be used.

4.4. The influence of shearing stress already present in the section before loading

From figure 3.4.1. it appears that shear stresses have an important influence if the shearing force does not reverse at the lateral compression force.

An explanation of this phenomenon is given in figure 4.4.1. The buckling caused by the shearing force is increased by the lateral compression force.



Shearing force reversal
Shearing force does not influence buckling

Continuous shearing force
Shearing force increases buckling

Figure 4.4.1.

The ultimate limit load calculated with formula (5) agrees with this situation.

4.5. Influence of tensile stress caused by bending already present before loading

These tests failed. The bending necessary to give sufficient bending before loading could not be maintained during the test. The beam inclined to collapse over the support with increasing lateral force. That is why the tensile stress is lower than 100 N/mm^2 .

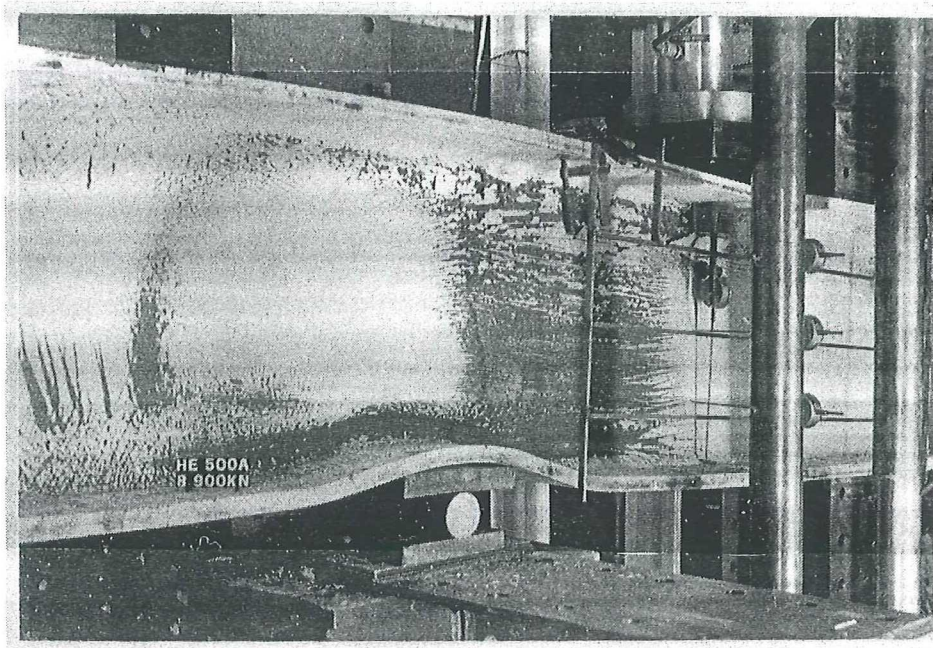
Other tests showed that the compression stress is more dangerous than the tensile stress and that the compression stress must be higher than 100 N/mm^2 .

See the results of tests 10, 11 and 12, figure 3.3.3.

The buckling appeared in the compression zone of these specimens

4.6. Specimens collapsed over the support

These specimens collapsed despite of the big plate (200 x 30 mm) used to spread the force at the support, see figure 4.6.1.



Collapse over the support despite
of the big plate to spread the force

Figure 4.6.1.

This collapse must be attributed to the interaction of bending and shearing stresses, where the latter influence was greater.

This fact may be concluded by comparing the collapse modes as shown in the photographs in figure 3.6.1.

Clearly formula (3) can only be used for concentrated forces and not for situations existent at the support at this case.

4.7. The influence of axial compression force already existent before loading

The results reported in figure 3.7.1. confirm completely with the statement that the collapse load of lateral compression forces is only influenced if the normal stress is higher than 100 N/mm^2 .

The part of formula (4) which reduces the ultimate limit force seems to be too conservative but can not be neglected

5. Conclusions

5.1. The collapse load of a lateral compression force is not influenced by local shearing stresses caused by the compression load itself.

This implies that the limit state of a connection can be calculated by considering three separated regions as stated in the introduction.

5.2. The collapse load of a lateral compression force is influenced by shearing stresses caused by other loads.

This can be taken into account with formula (5)

$$\hat{F} = \sigma_e t_{wC} \{ t_{fb} + 5(r_c + t_{fc}) \} * \sqrt{1 - \frac{3\tau^2}{\sigma_e^2}} \quad (5)$$

5.3. The collapse load of a lateral compression force is influenced by axial force and bending moments.

This can be taken into account with formula (4).

$$\hat{F} = \sigma_e t_{wC} \{ t_{fb} + 5(r_c + t_{fc}) \} * (1,25 - 0,5 \frac{|\sigma|}{\sigma_e}) \quad (4)$$

$$1,25 - 0,5 \frac{|\sigma|}{\sigma_e} \leq 1$$

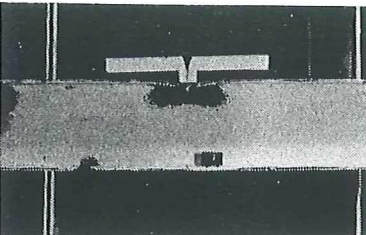
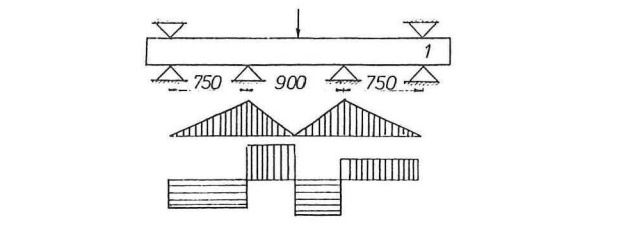
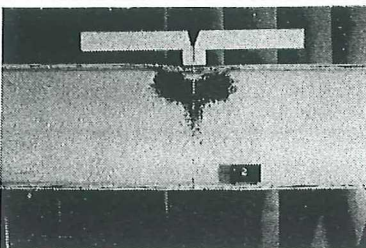
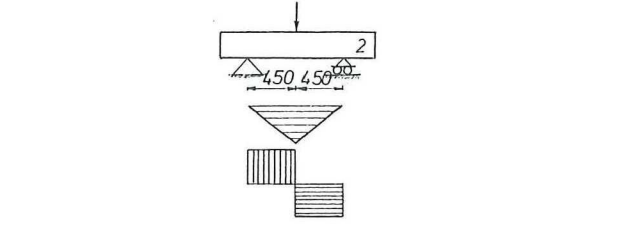
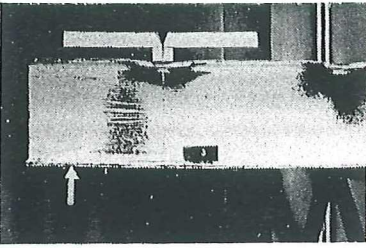
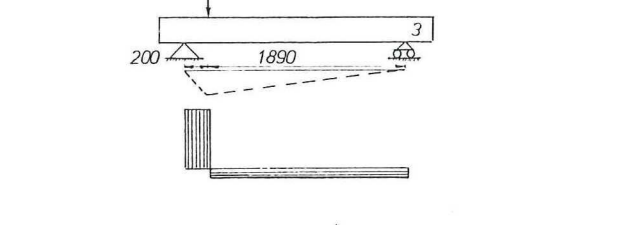
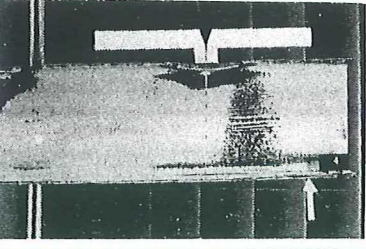
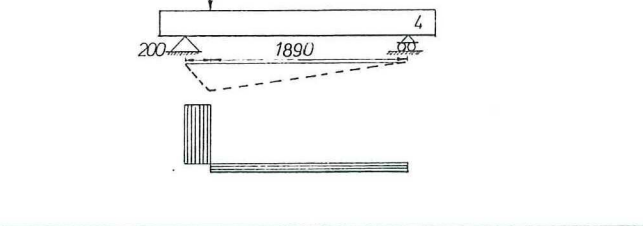
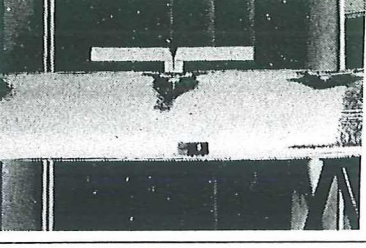
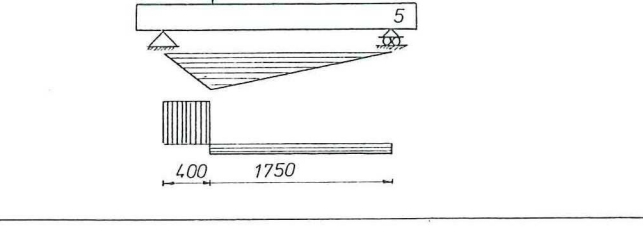
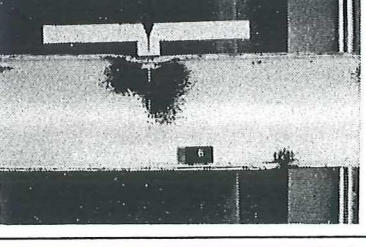
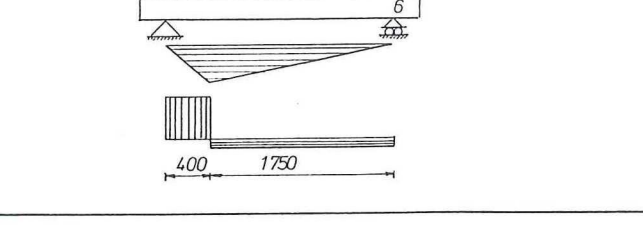
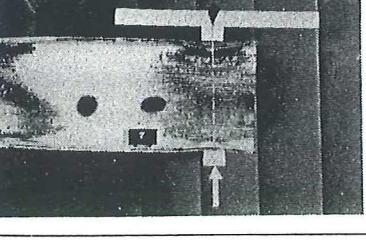
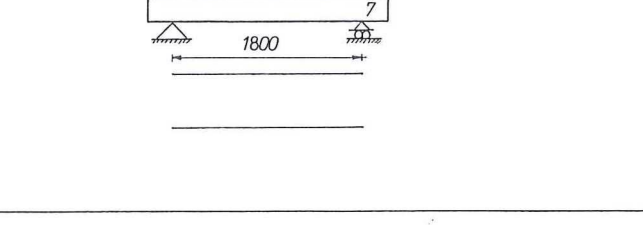
and σ = summation of stresses caused by bending and normal force in the very edge of the section.

6. Literature

- |1| Bakker C.Th.J. and W.J.M Voorn
"Welded beam-to-column connections in frames"
(in Dutch)
Agon Elsevier, Amsterdam/Brussel 1974
- |2| "Steifenlose Stahlskelettragwerke and dünnwandige
Vollwandträger - Berechnung and Konstruktion",
Europäische Empfehlungen - EGKS,
Verlag von Wilhelm Ernst & Sohn,
Berlin - München - Düsseldorf, 1977.

IPE 240

 $\sigma_y = 367 \text{ N/mm}^2$ $\tau_y = 213 \text{ N/mm}^2$

Photographs of collapsed specimens	Test set-up Bending moment - diagram. Shearing force diagram.	$F_{\text{buckl.}}$ kN	$\sigma_{\text{br.2}}$ N/mm ²	$\tau_{\text{br.2}}$ N/mm ²	$\tau_{\text{br.1}}$ N/mm ²
		380	0	139	139
		349	192	128	128
		350	n.v.t.	232	24
		350	n.v.t.	232	24
		283	225	168	38
		280	223	166	38
		380	0	0	0

IPE 240

$\sigma_y = 367 \text{ N/mm}^2$ $\tau_y = 213 \text{ N/mm}^2$

Photographs of collapsed specimens	Test set-up Bending moment - diagram. Shearing force diagram.	$F_{\text{buckl.}}$ kN	$\sigma_{\text{pr.2}}$ N/mm ²	$\tau_{\text{pr.2}}$ N/mm ²	$\tau_{\text{pr.2}}$ N/mm ²
		380	0	0	321
		310	n.v.t.	200	27
		340	139	0	0
		335	185	0	0
		375	92,5	0	0
		380	0	0	0
		350	113,8	113,4	113,4

IPE 240

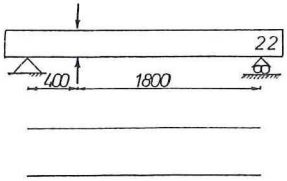
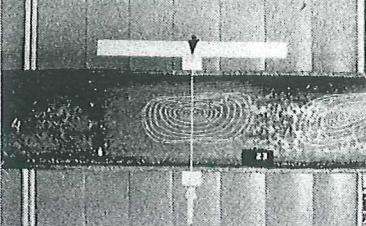
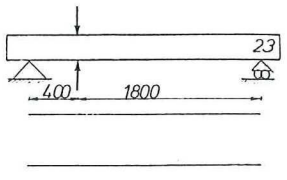
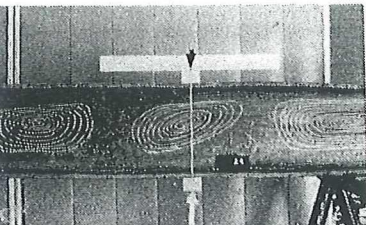
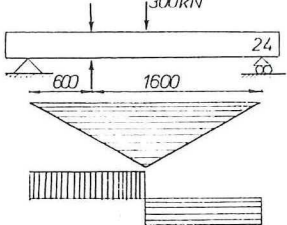
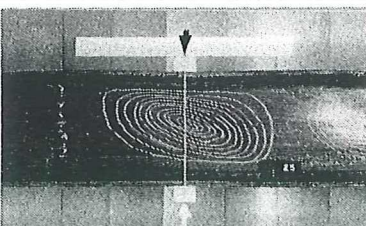
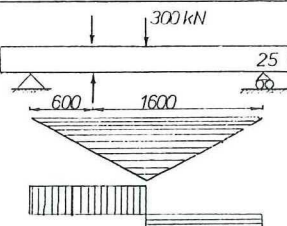
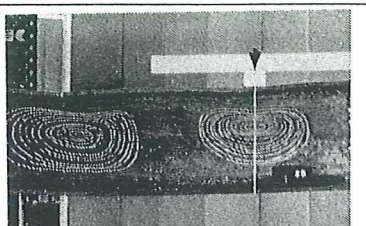
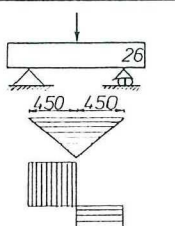
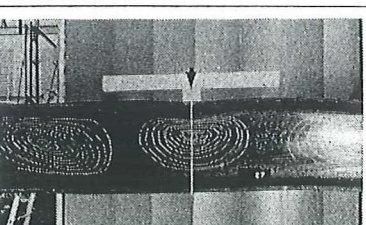
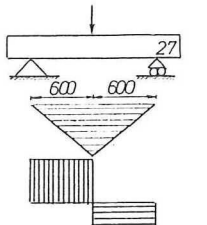
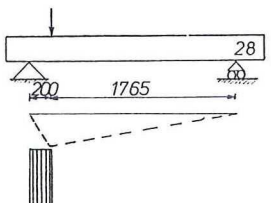
$\sigma_y = 425 \text{ N/mm}^2$

$\tau_y = 247 \text{ N/mm}^2$

Photographs of collapsed specimens	Test set-up Bending moment-diagram. Shearing force diagram.	$F_{buckl.}$ kN	$\sigma_{n.pr.}$ N/mm	$\tau_{l.pr.}$ N/mm	$\tau_{r.pr.}$ N/mm
		200	242	0	0
		283	242	0	0
		322	102	0	0
		340	0	0	0
		300	0	0	0
		330	0	0	0
		320	0	0	0

HE 240 A

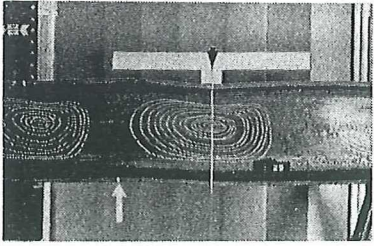
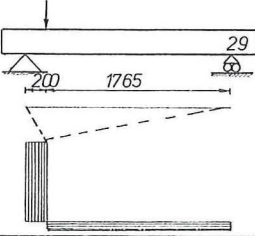
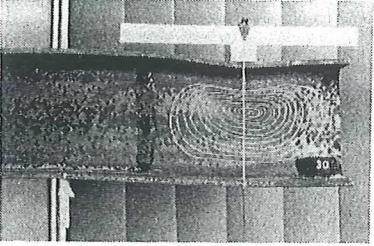
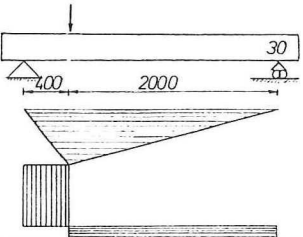
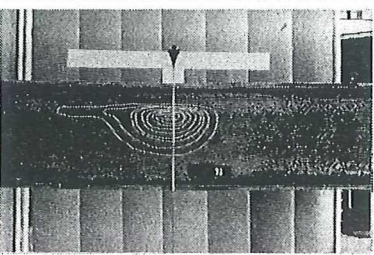
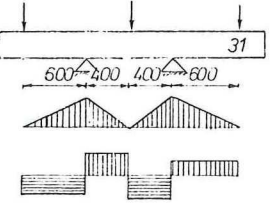
$\sigma_y = 317 \text{ N/mm}^2$ $\tau_y = 184 \text{ N/mm}^2$

Photographs of collapsed specimens	Test set-up Bending moment - diagram. Shearing force diagram.	F_{buckl} kN	$\sigma_{b,pr}$ N/mm ²	$\tau_{l,pr}$ N/mm ²	$\tau_{r,pr}$ N/mm ²
		483	0	0	0
		483	0	0	0
		380	92,5	92,6	92,6
		385	92,5	92,6	92,6
		480	114	155	155
		458	14,5	14,8	14,8
		488	n.v. t.	283	33

HE 240 A

$\sigma_y = 317 \text{ N/mm}^2$

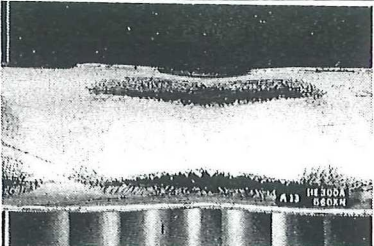
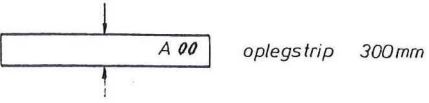
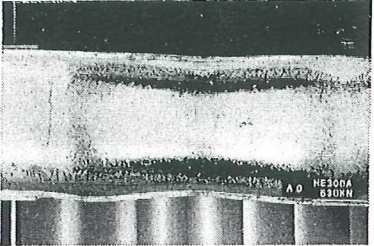
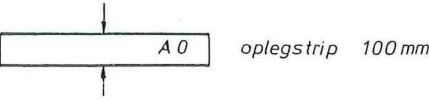
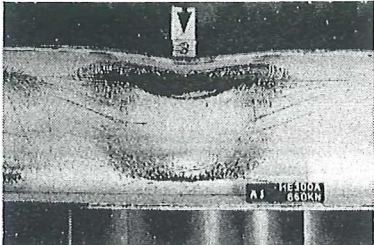
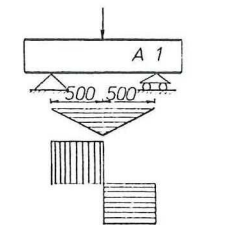
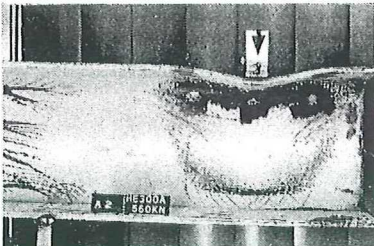
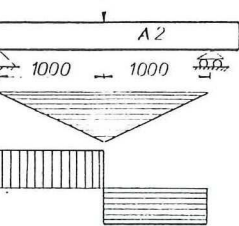
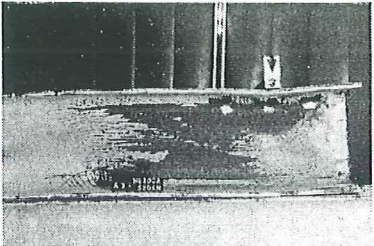
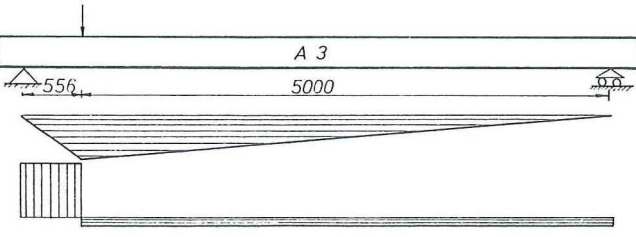
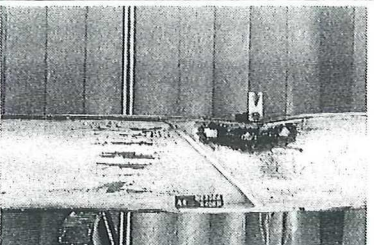
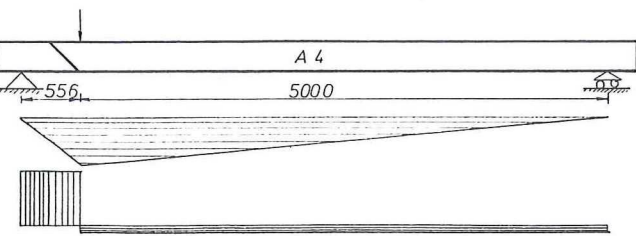
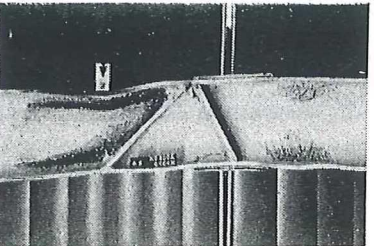
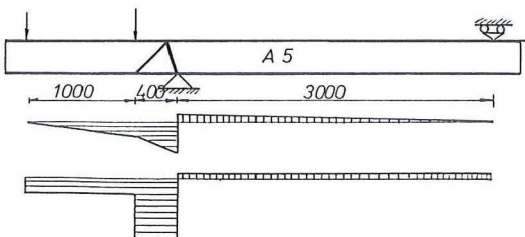
$\tau_y = 184 \text{ N/mm}^2$

Photographs of collapsed specimens	Test set-up Bending moment-diagram. Shearing force diagram.	F_{buckl} kN	$\sigma_{bpr.2}$ N/mm ²	$\tau_{lpr.2}$ N/mm ²	$\tau_{rpr.2}$ N/mm ²
		480	n.v.t.	279	31
		429	151	231	46
		473	0	153	153

HE 300 A

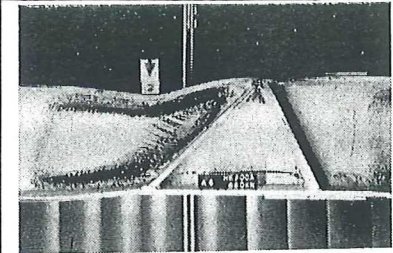
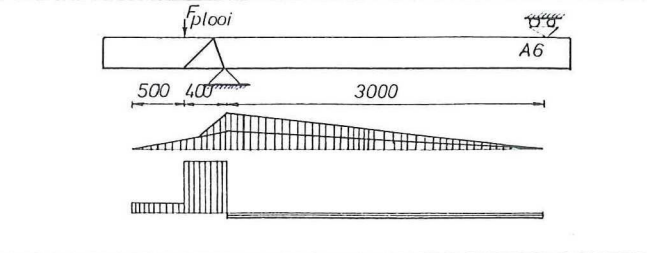
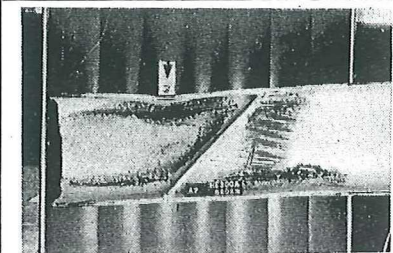
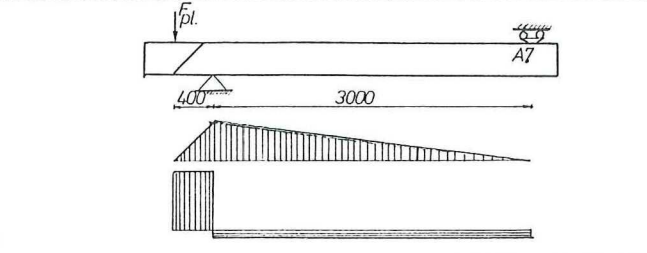
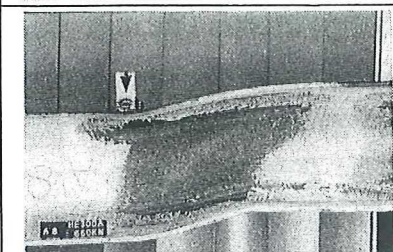
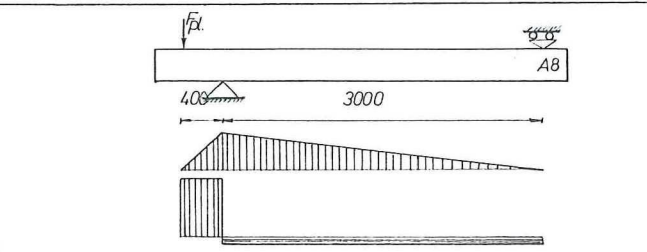
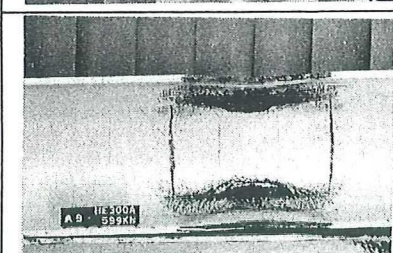
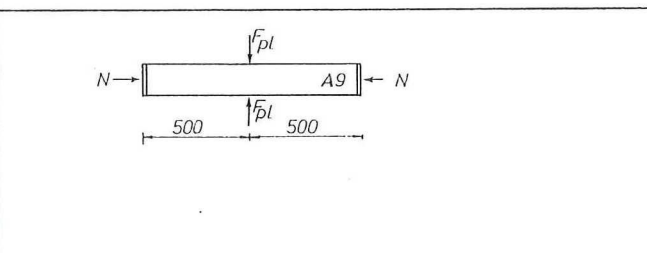
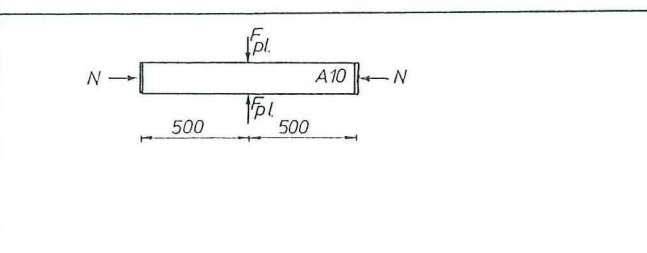
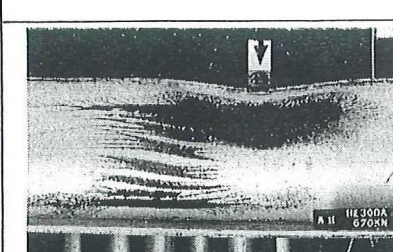
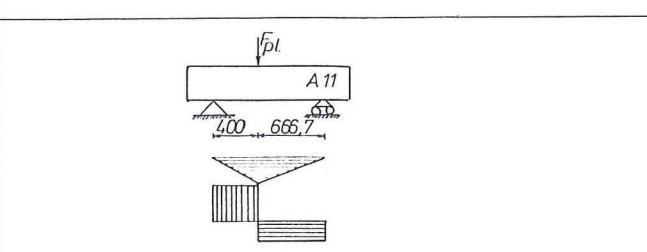
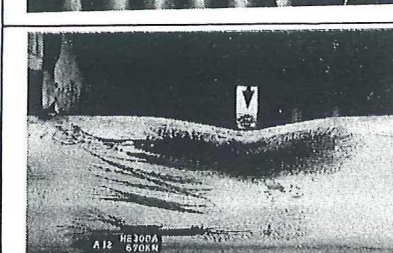
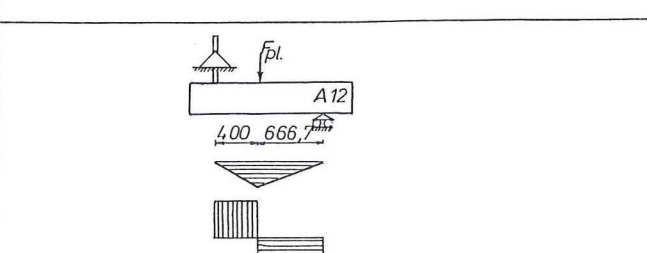
$\sigma_y = 357 \text{ N/mm}^2$

$\tau_y = 207 \text{ N/mm}^2$

Photographs of collapsed specimens	Test set-up Bending moment - diagram. Shearing force diagram.	F_{buckl} kN	σ_{bpr} N/mm ²	τ_{lpr} N/mm ²	τ_{rpr} N/mm ²
		660			
		630			
		660	108	149	149
		560	183	126	126
		520	170	210	23,4
		540	177	(219)	24
		650	55	38	(330)

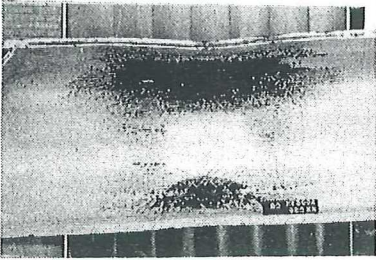
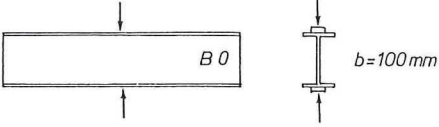
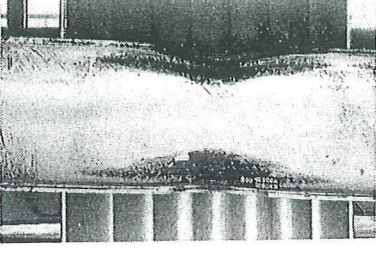
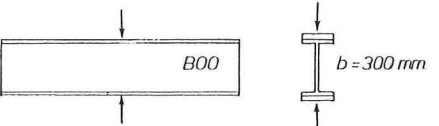
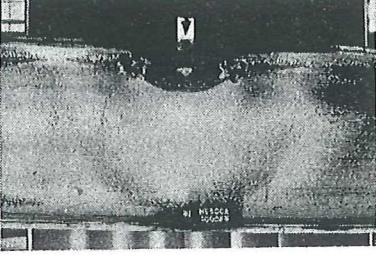
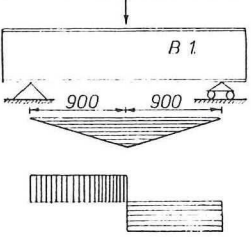
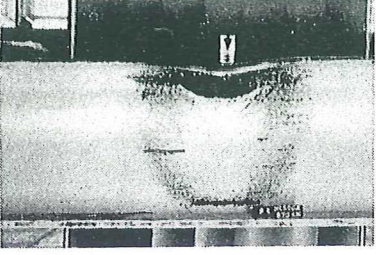
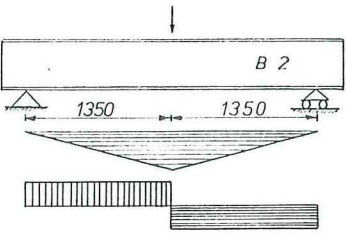
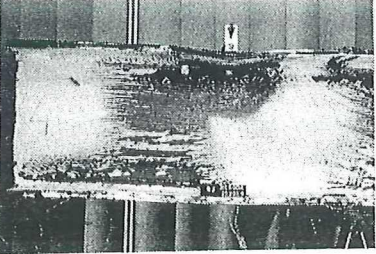
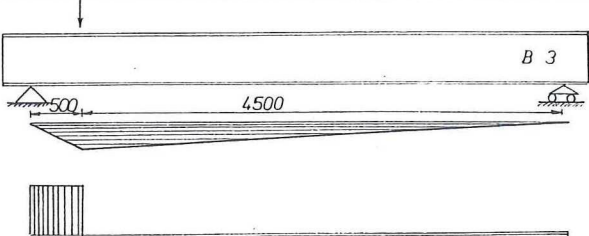
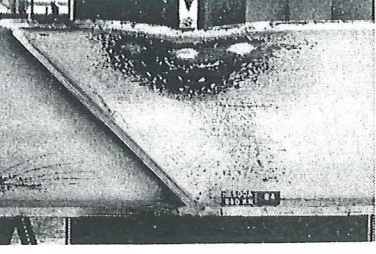
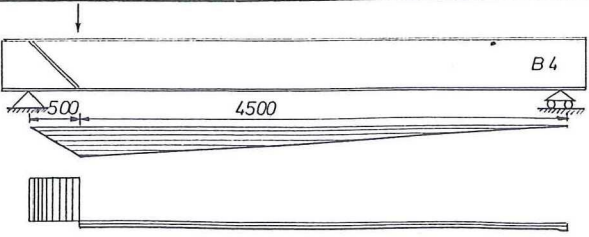
HE 300 A

 $\sigma_y = 357 \text{ N/mm}^2$ $\tau_y = 207 \text{ N/mm}^2$

Photographs of collapsed specimens	Test set-up Bending moment - diagram. Shearing force diagram.	$F_{\text{buckl.}}$ kN	$\sigma_{\text{bpr.}}$ N/mm ²	$\tau_{\text{Ipr.}}$ N/mm ²	$\tau_{\text{pr.}}$ N/mm ²
		660	27,5	(340)	39
		680	0	(310)	
		660	0	310	
		599	$\sigma_{\text{pr.}}$ 173		
		682	$\sigma_{\text{pr.}}$ 109		
		670	110	191	114
		670	110	191	114

HE 500A

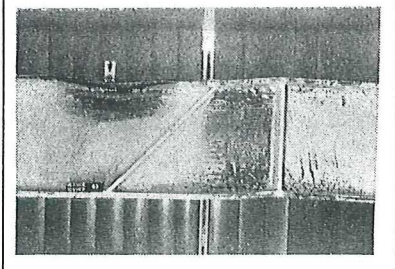
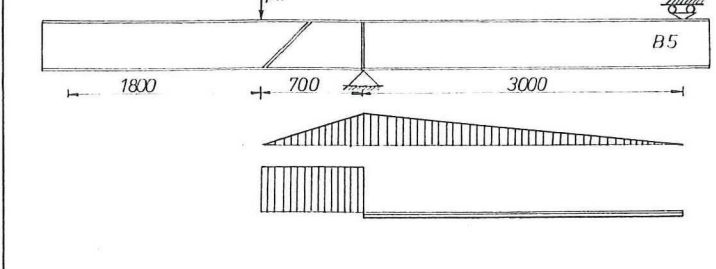
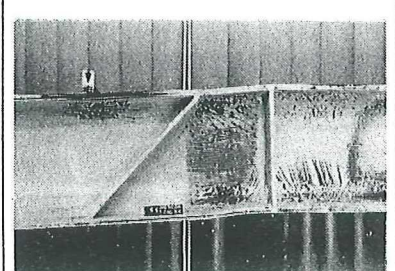
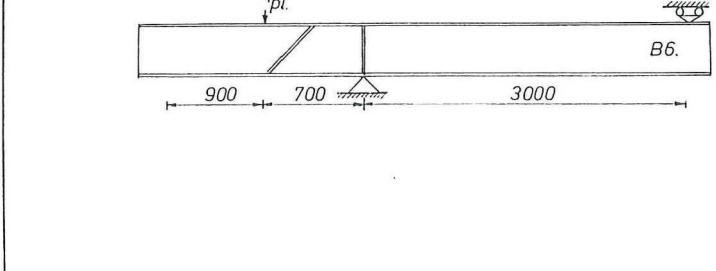
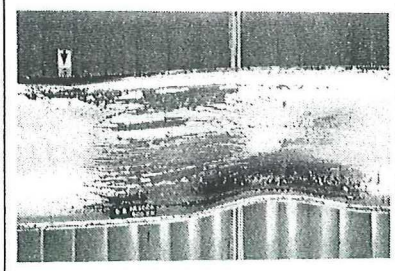
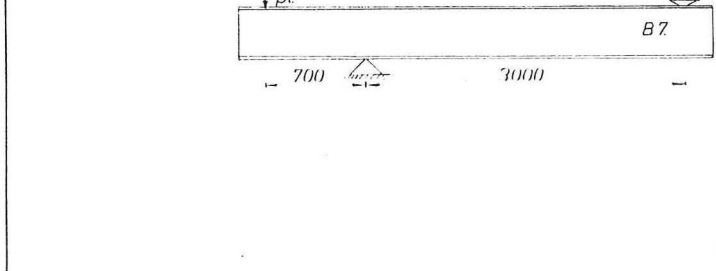
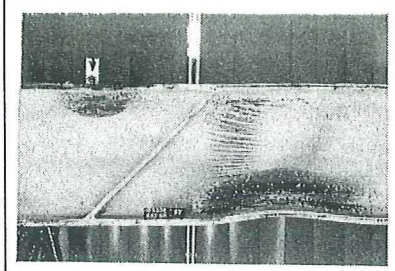
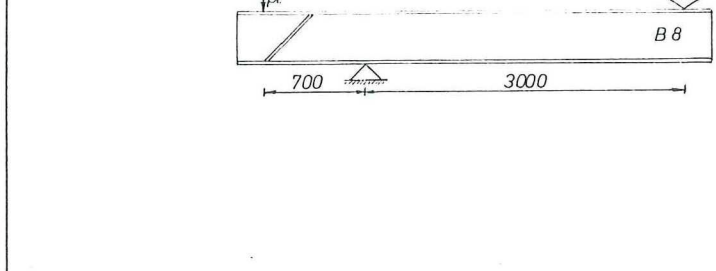
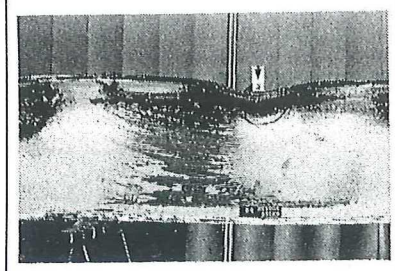
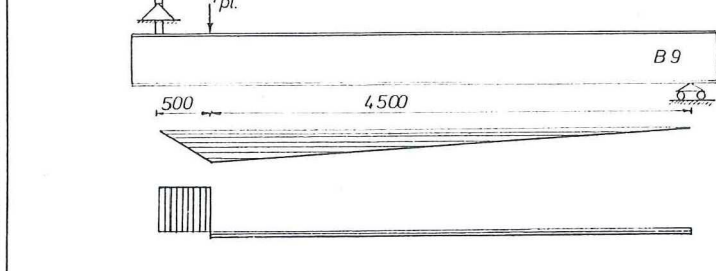
 $\sigma_y = 286 \text{ N/mm}^2$ $\tau_y = 166 \text{ N/mm}^2$

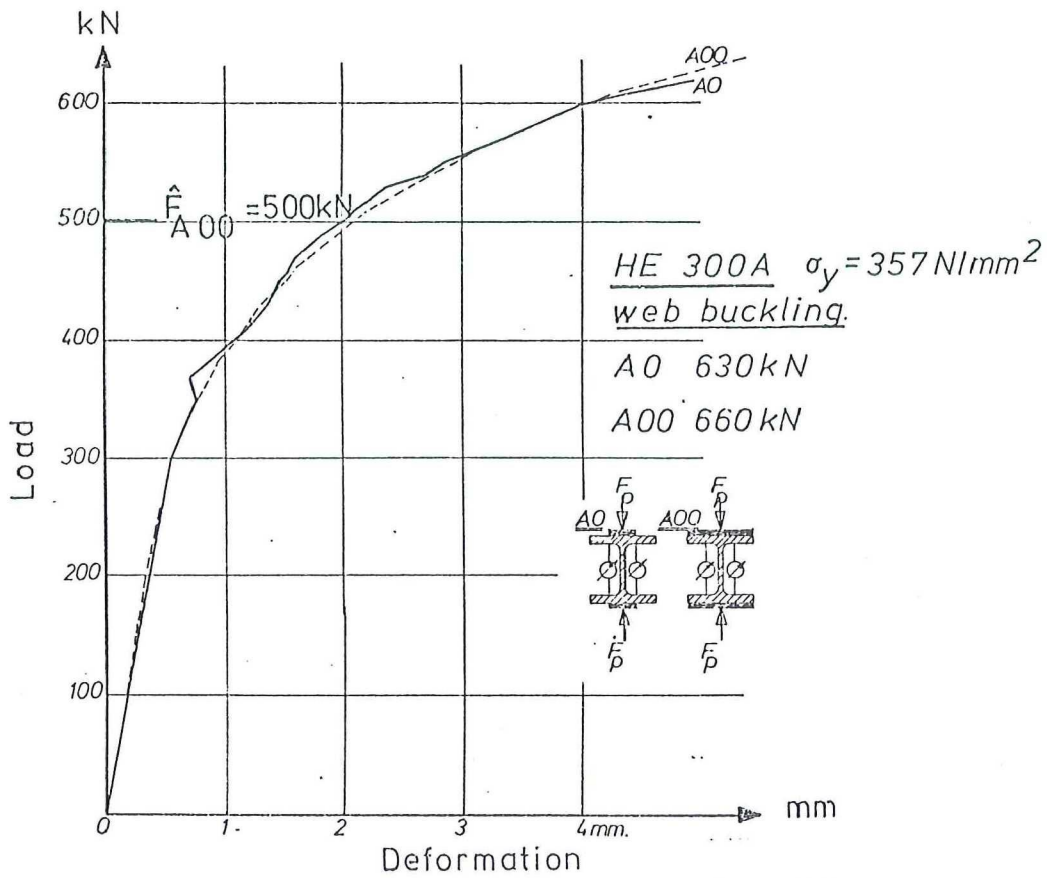
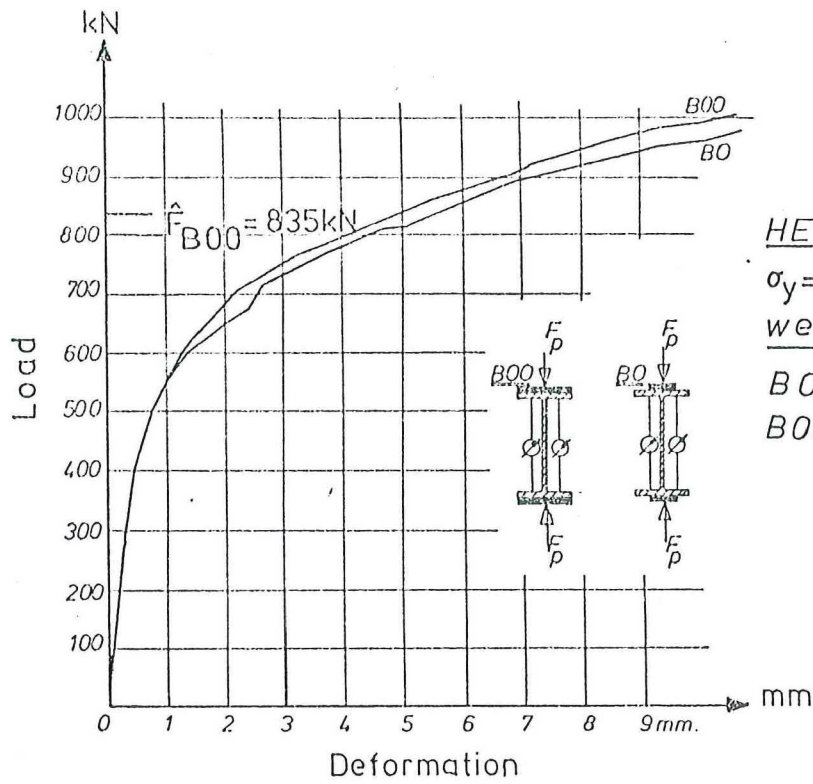
Photographs of collapsed specimens	Test set-up Bending moment - diagram. Shearing force diagram.	$F_{\text{buckl.}}$ kN	$\sigma_{b,pr}$ N/mm ²	$\tau_{l,pr}$ N/mm ²	τ_{pr} N/mm ²
		980	0	0	0
		1080	0	0	0
		1000	110	89	89
		870	143	78	78
		1030	113	166	18
		960	105	(154)	17

HE 500A

$\sigma_y = 286 \text{ N/mm}^2$

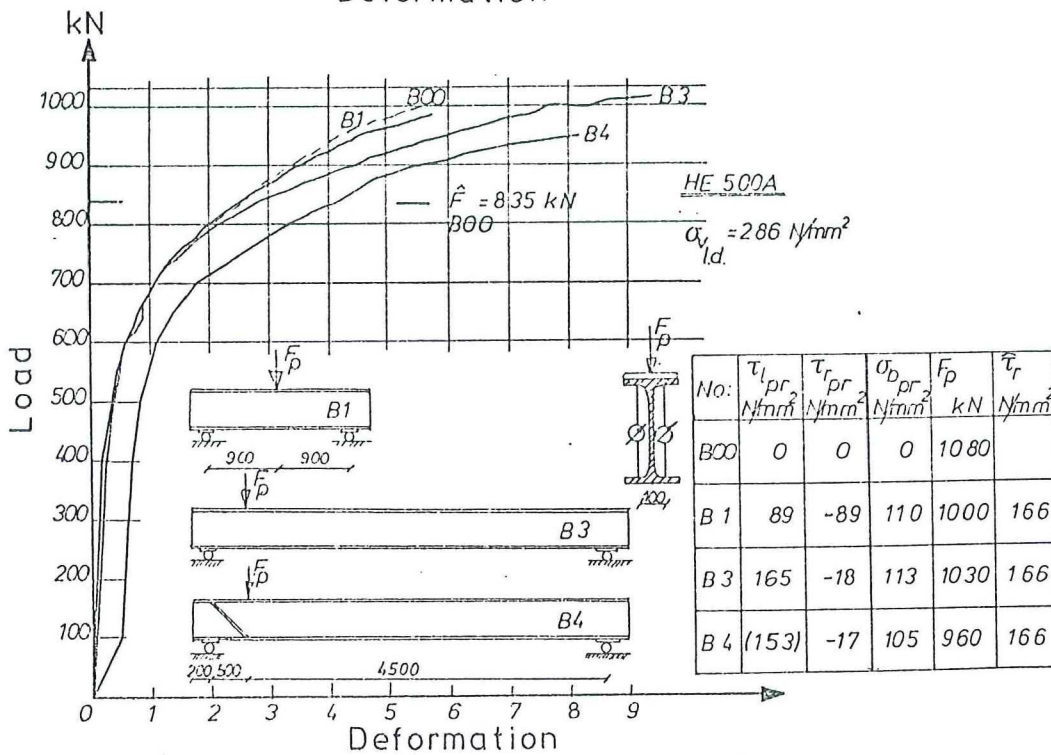
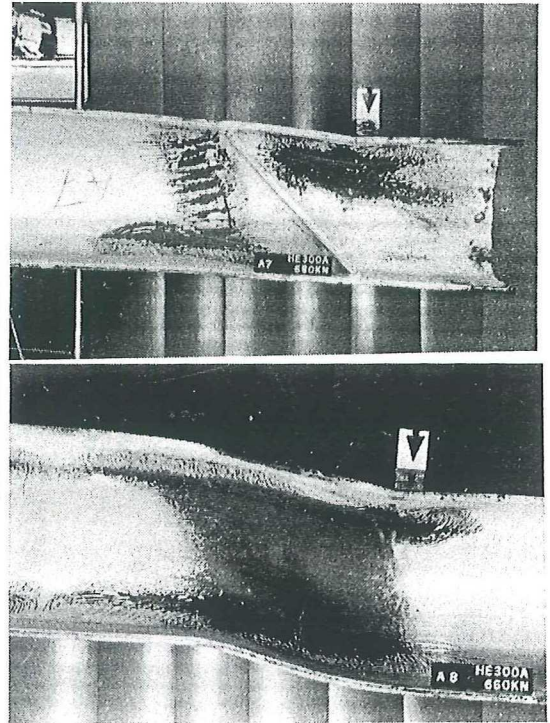
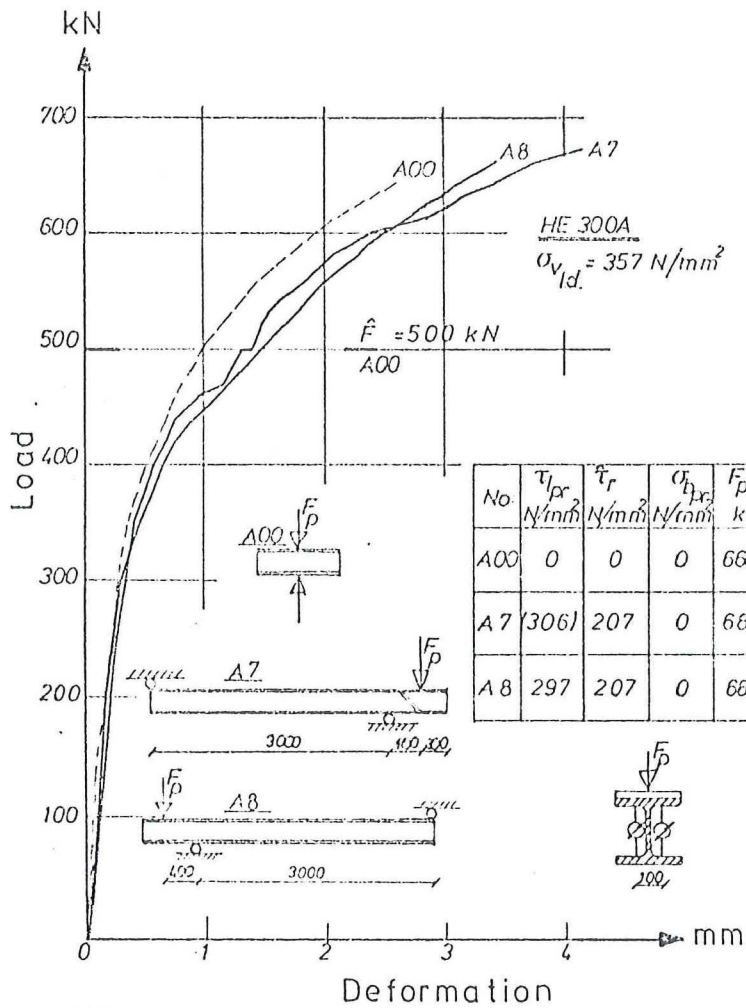
$\tau_y = 166 \text{ N/mm}^2$

Photographs of collapsed specimens	Test set-up Bending moment - diagram. Shearing force diagram.	$F_{buckl.}$ kN	$\sigma_{bpr.}$ N/mm ²	$\tau_{lpr.}$ N/mm ²	$\tau_{rpr.}$ N/mm ²
		1090	0	194	0
		(740) supp. 912		132	
		(880) supp. 1085		156	
		(900) supp. 1110		160	
		995	109	160	18



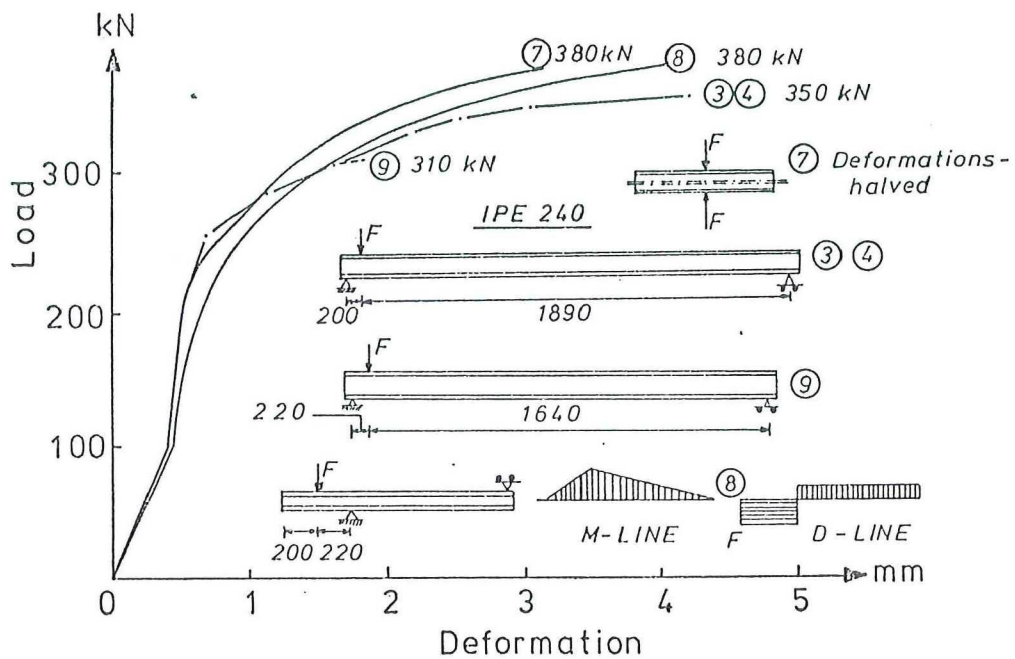
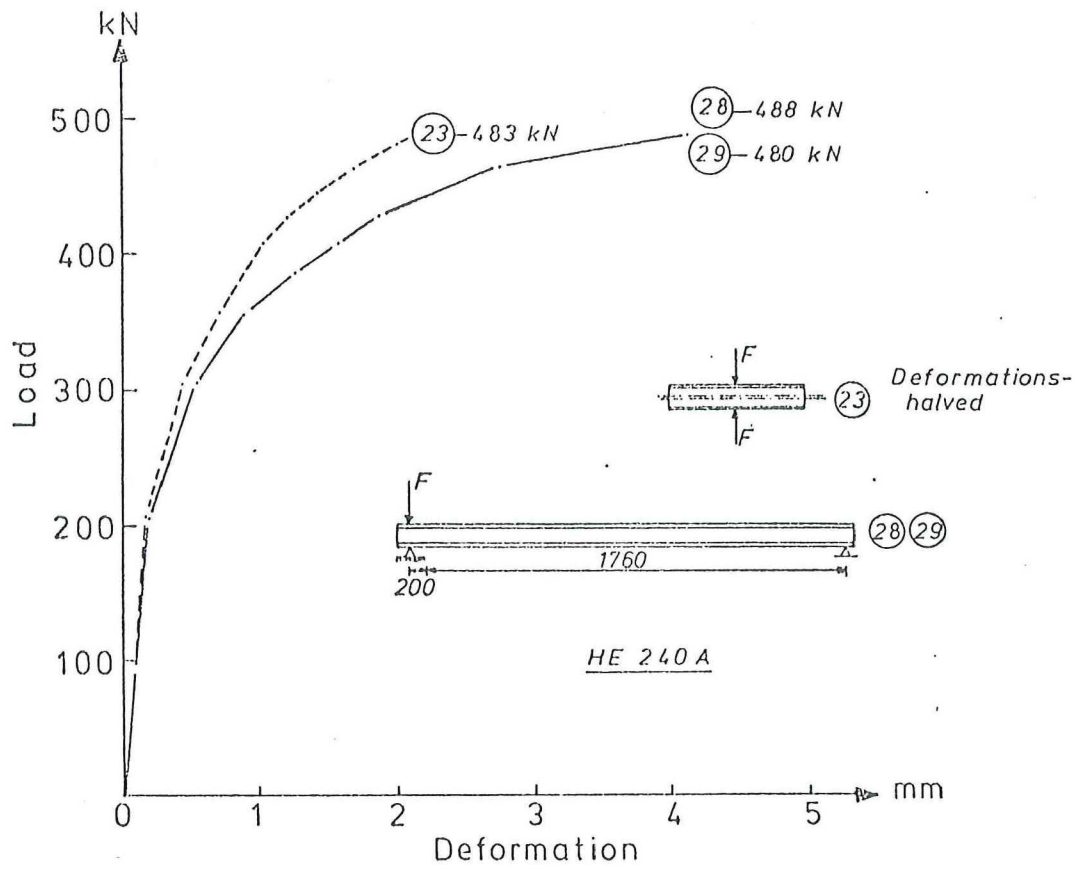
Influence of the length of loading-strip.

Figure. 3.1.1



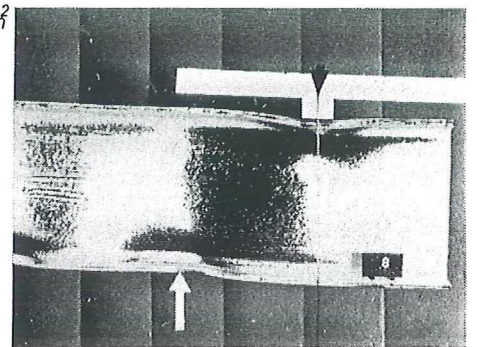
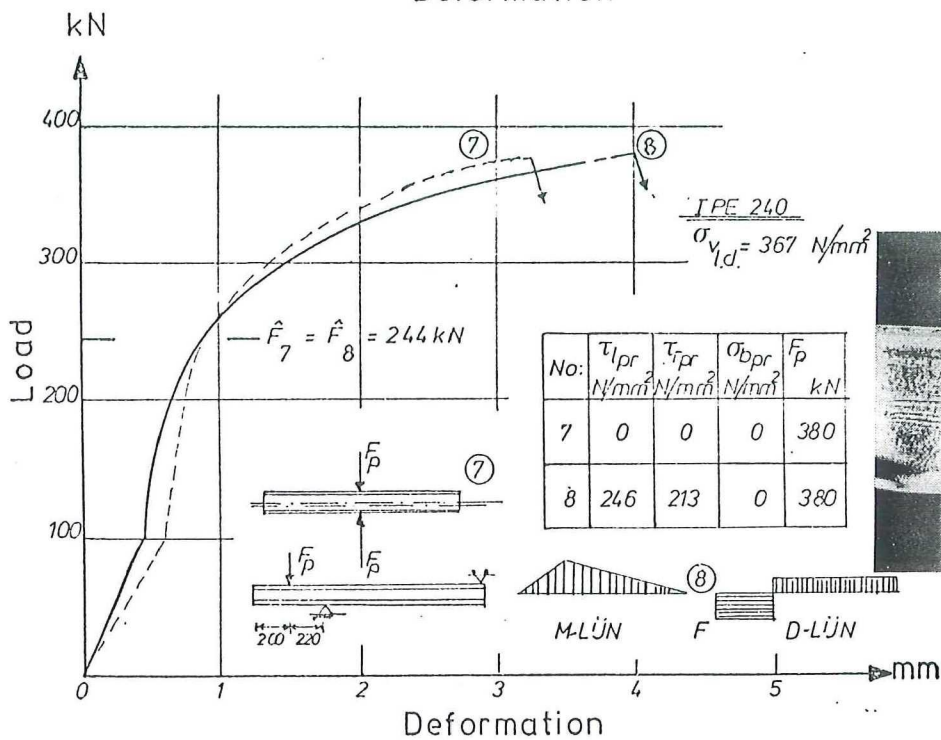
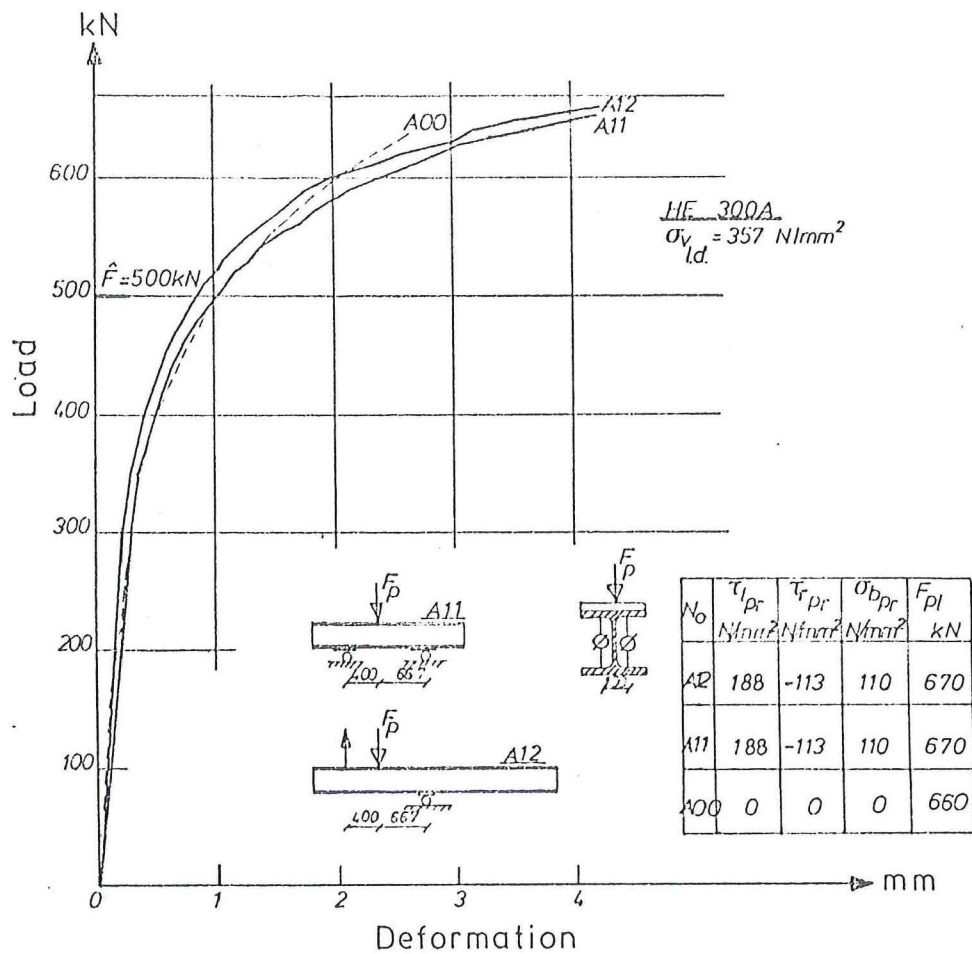
Influence of the shearing force caused by the lateral force itself. (with or without stiffener)

Figure. 3.2.1



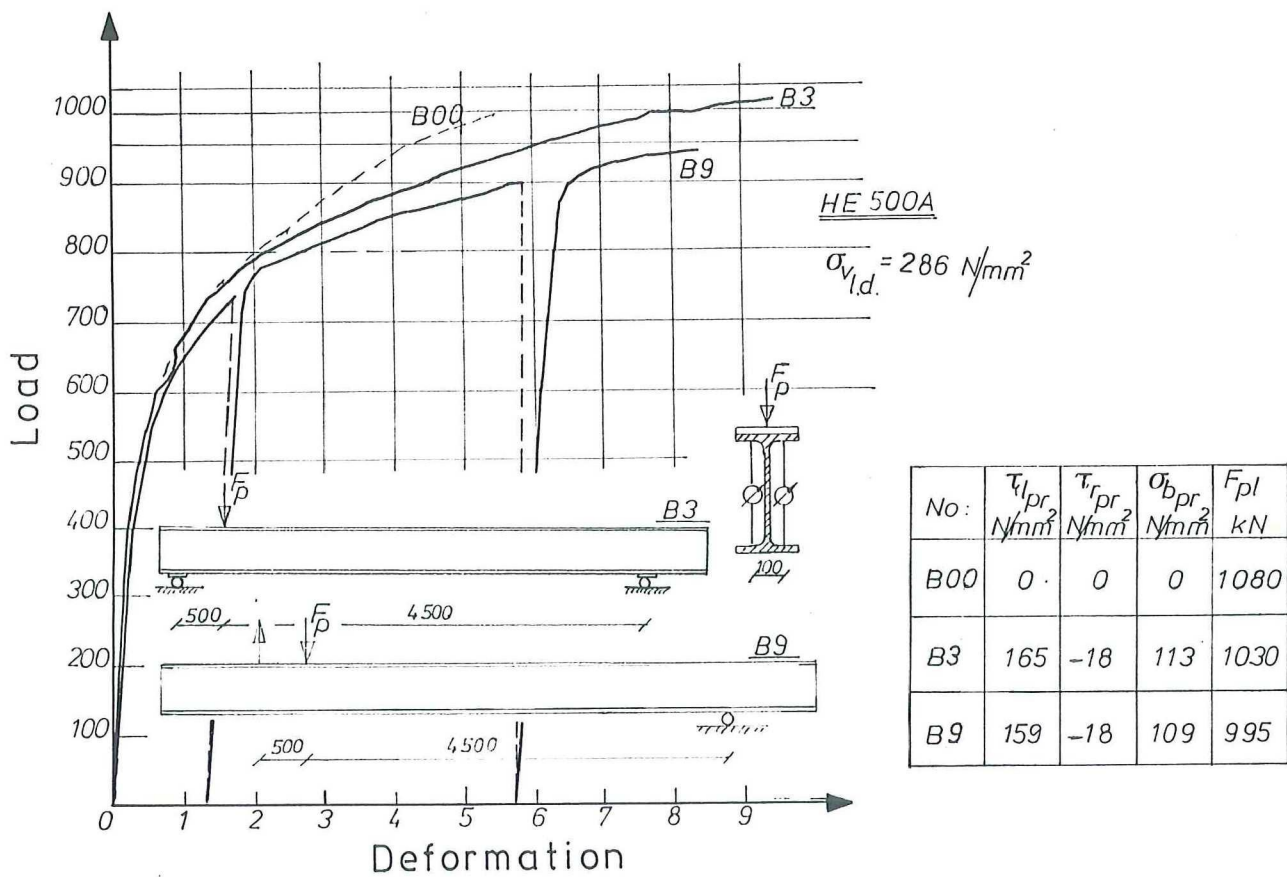
Influence of the shearing force caused by the lateral force itself (high shearing stress) (low bending stress)

Figure. 3.2.2



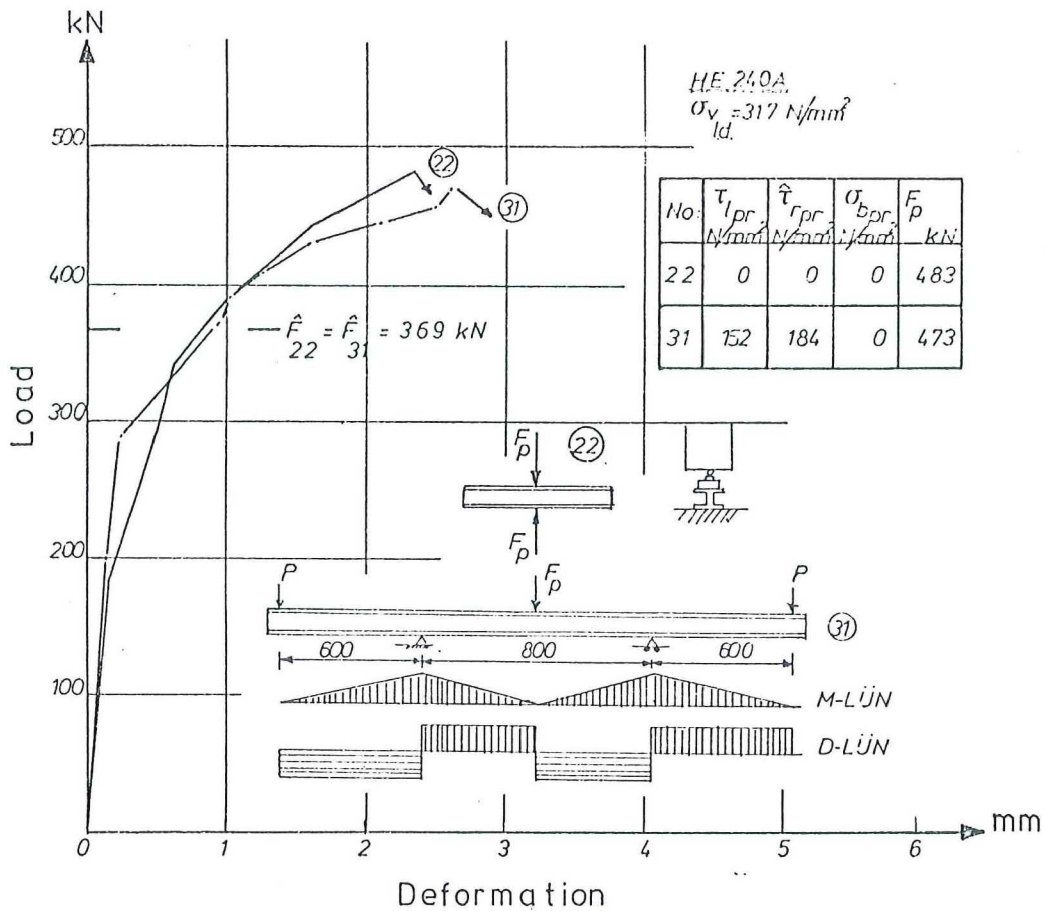
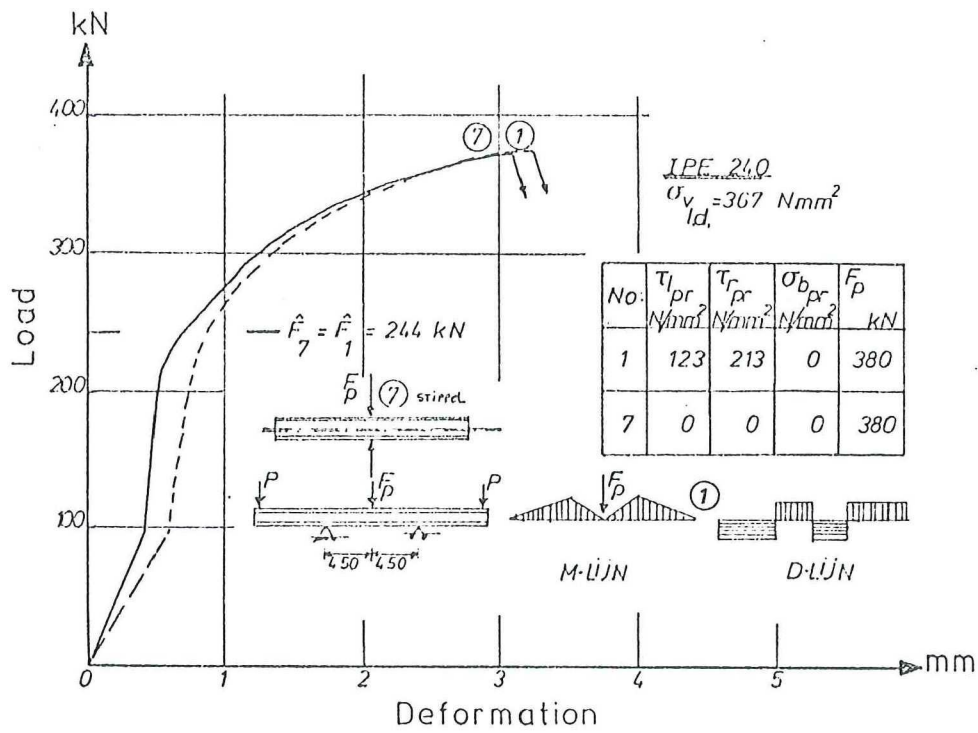
Influence of the shearing force caused by the lateral force itself. (high shearing stress)
 (low bending stress)

Figure. 3.2.3



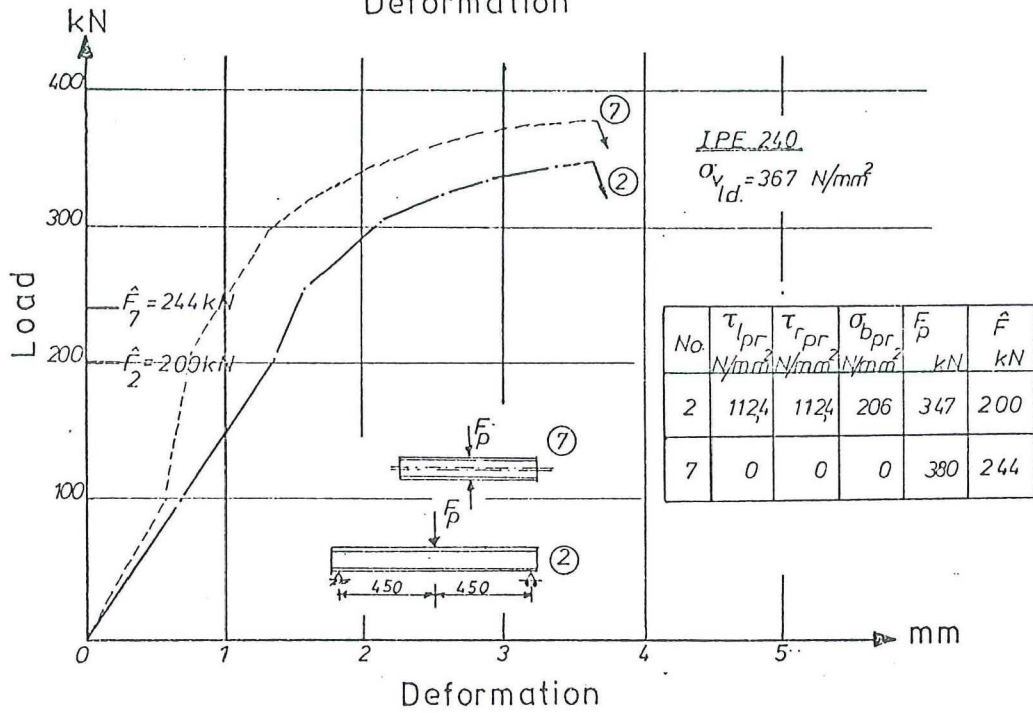
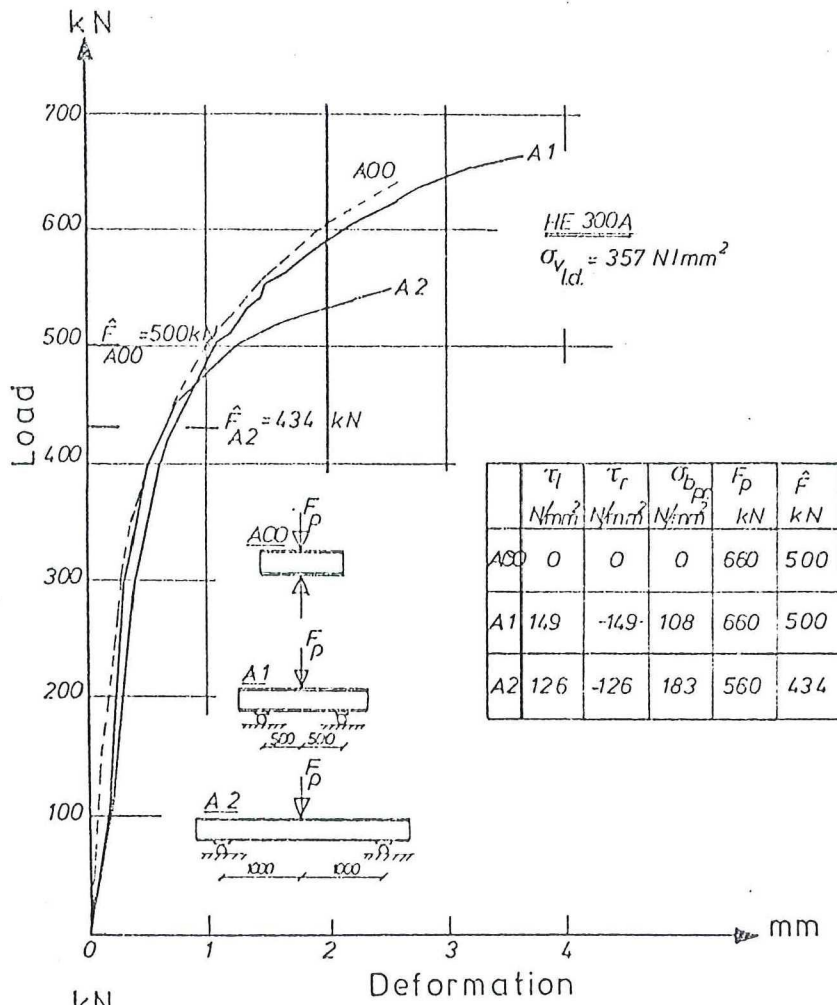
Influence of the shearing force caused by
the lateral force itself (high shearing stress)
(low bending stress)

Figure. 3.2.4



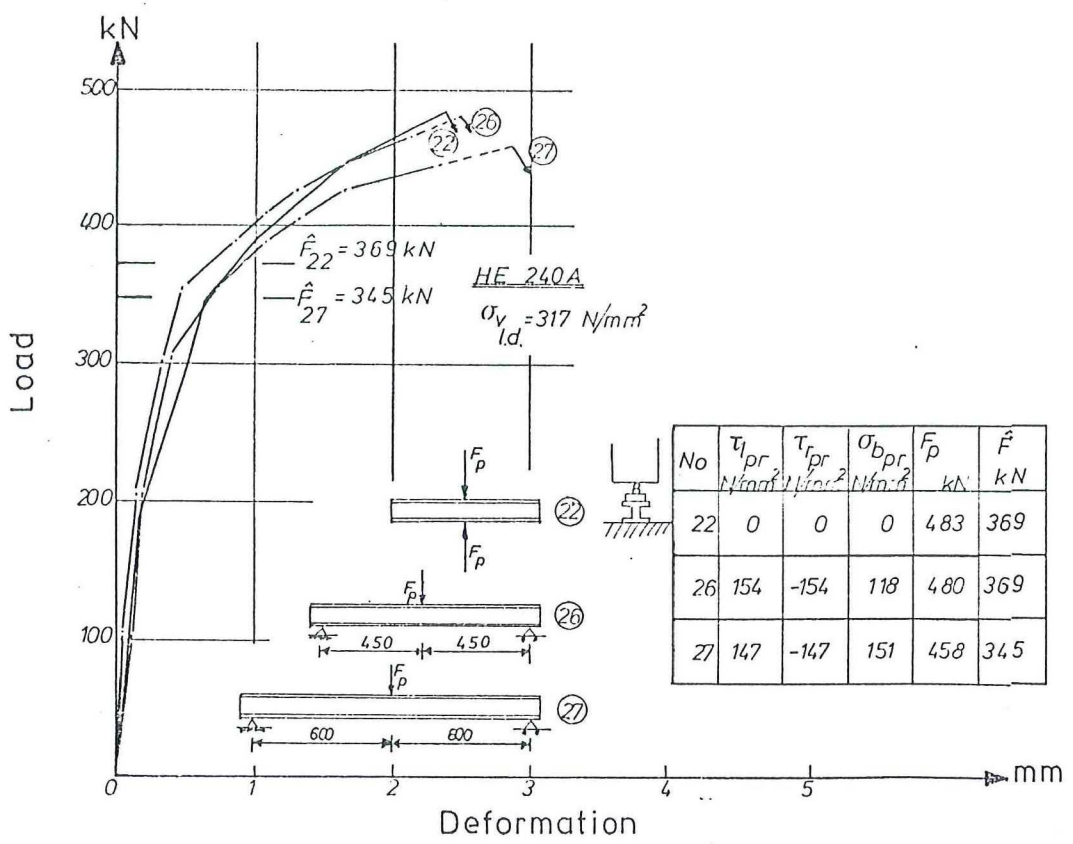
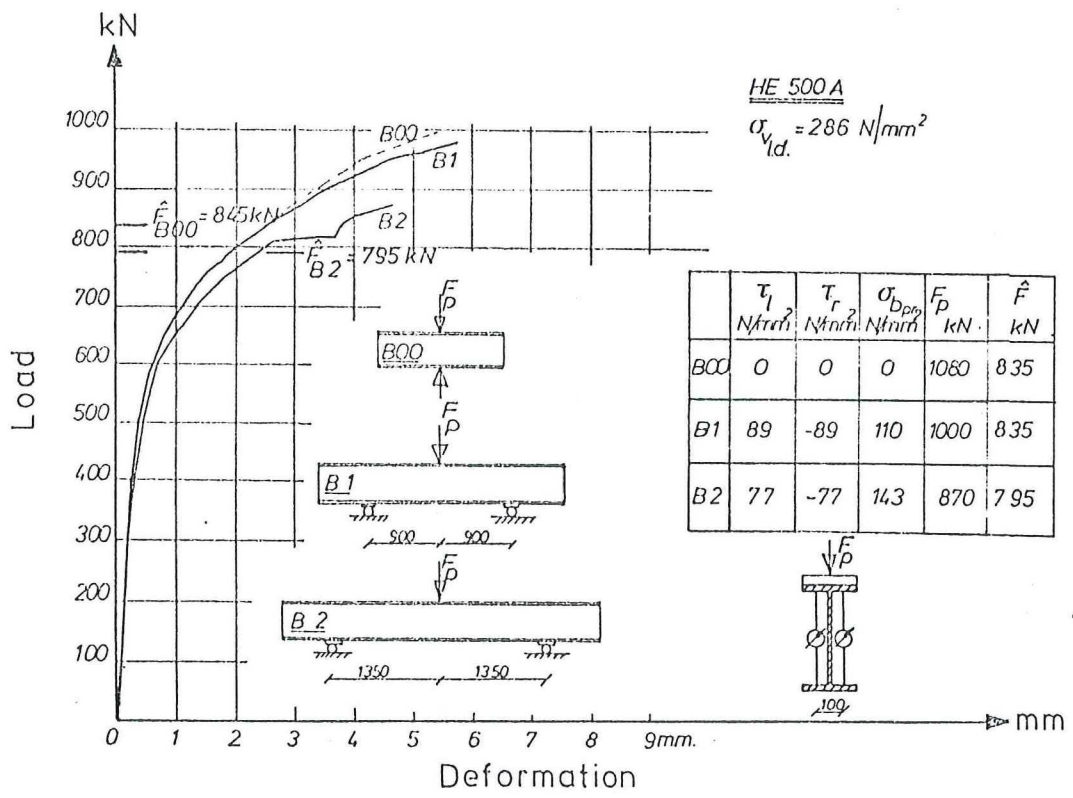
Influence of the shearing force caused by the lateral force itself. (no bending)

Figure.3.2.5

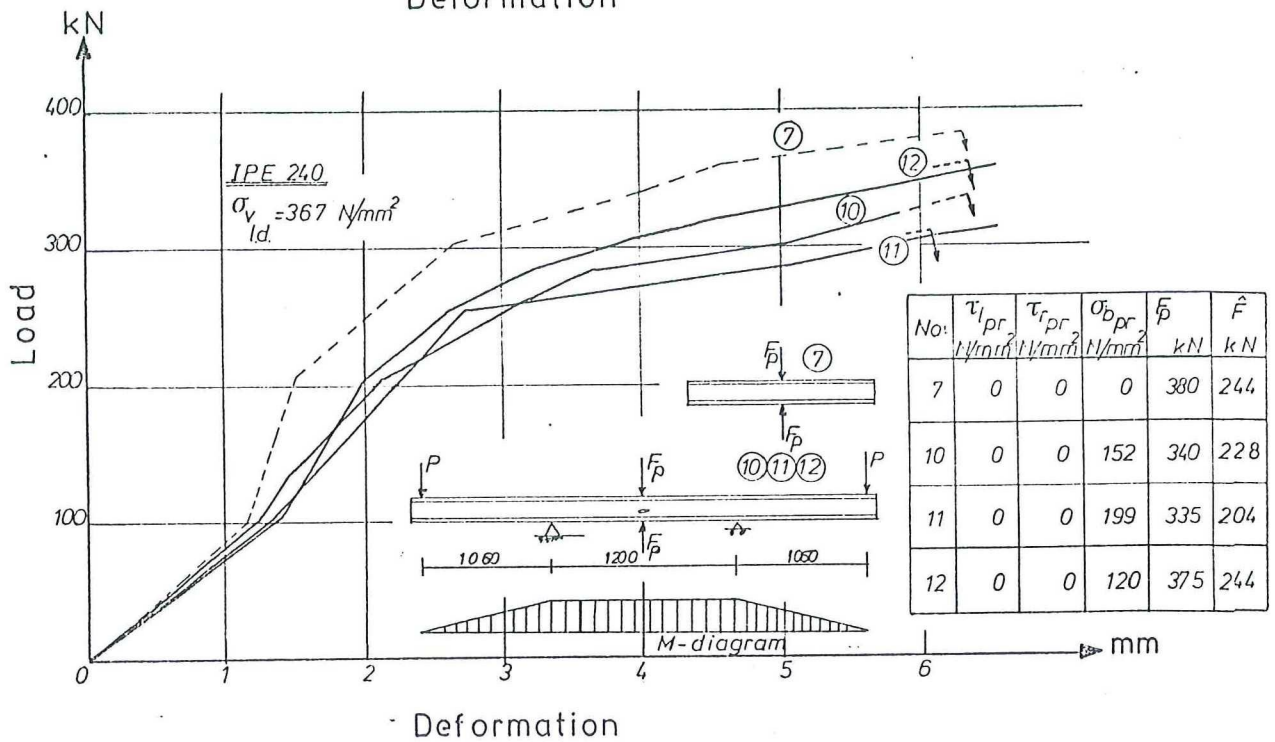
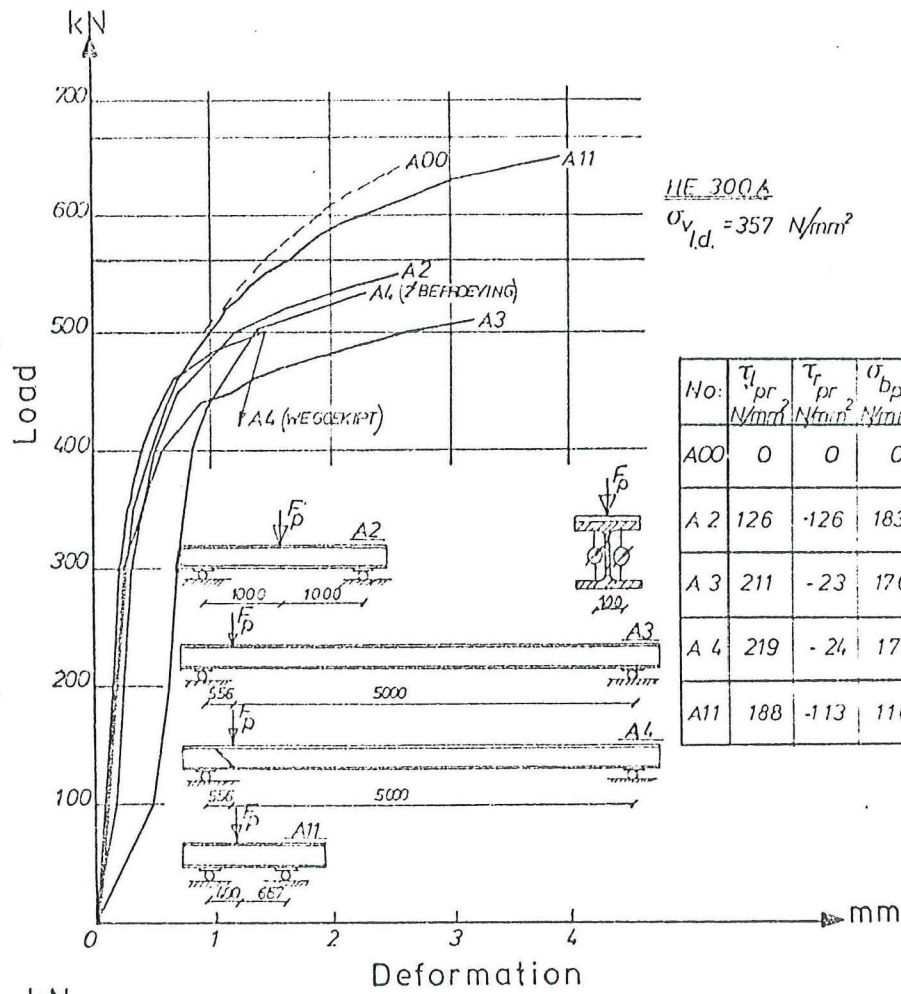


Influence of the bending stress (high and low bending stress)

Figure. 3.3.1



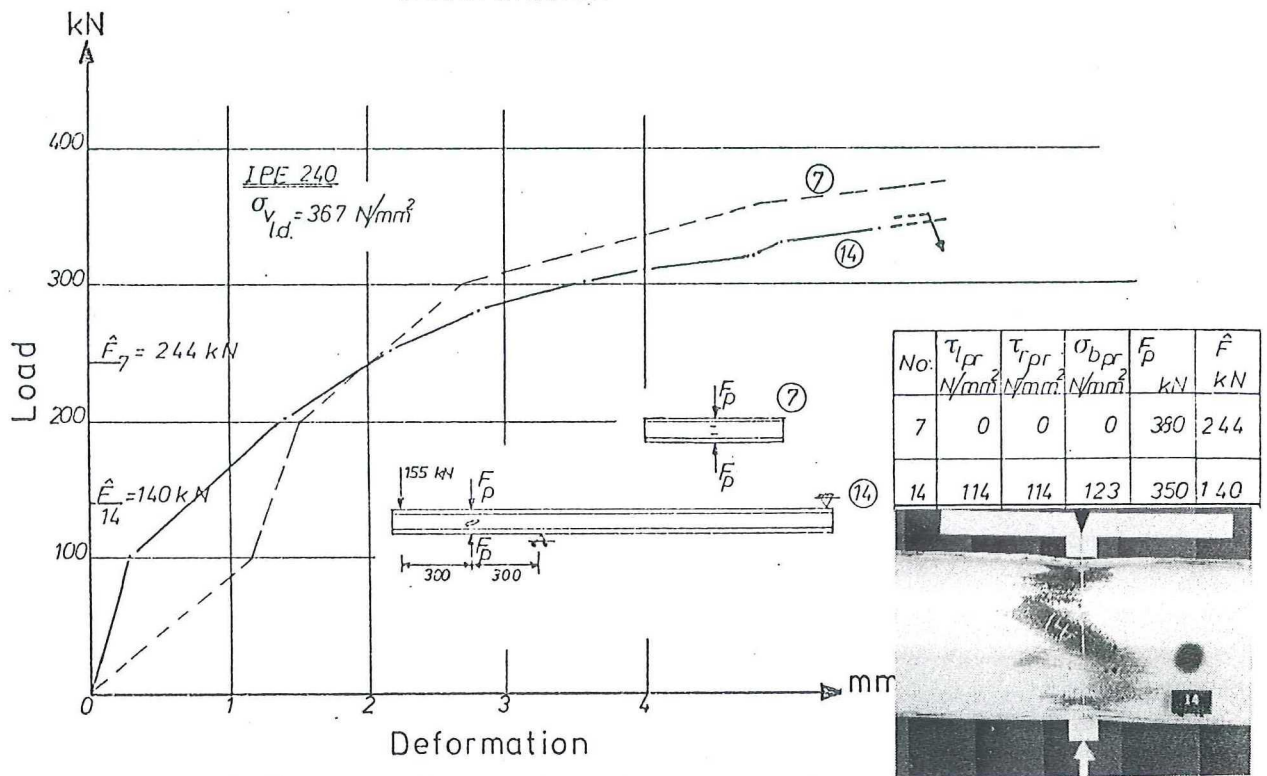
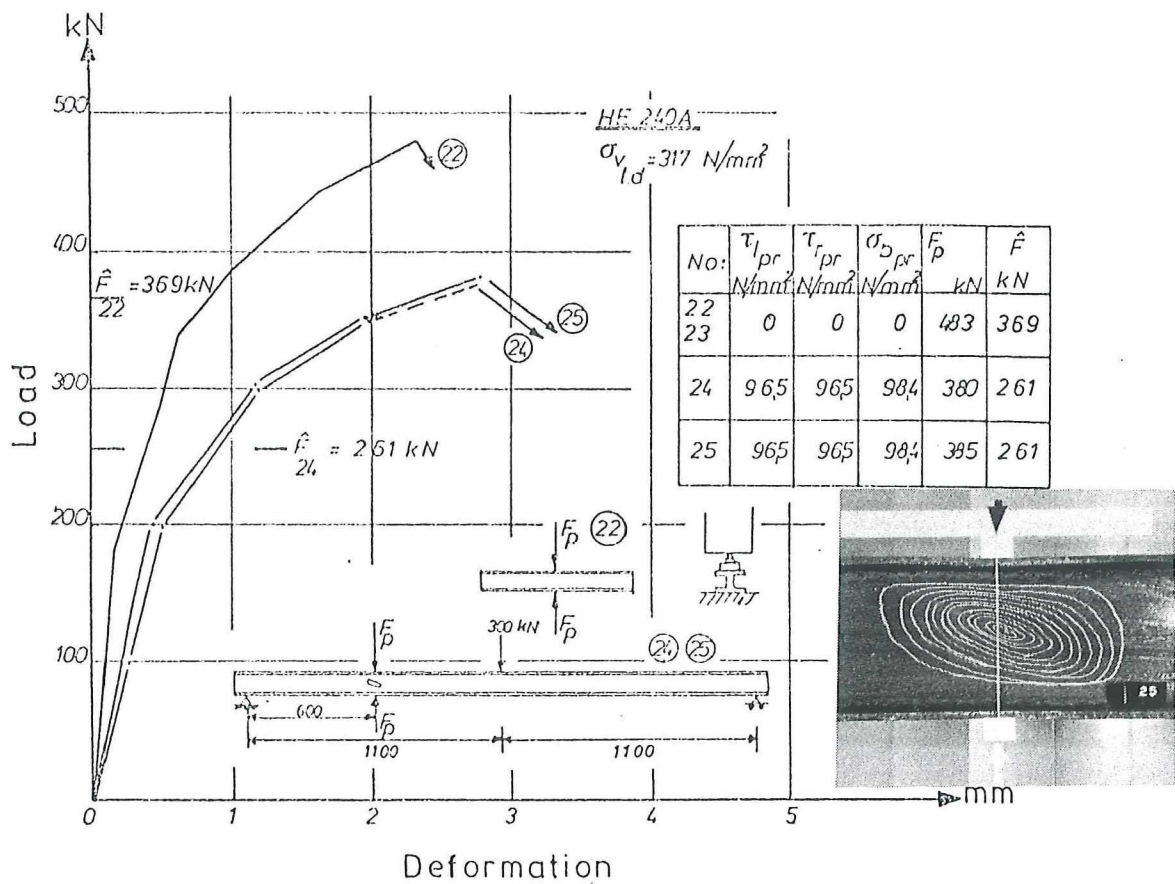
Influence of the bending stress (high and low bending stress)
 Figure. 3.3.2



Influence of the bending stress (high bending stress)

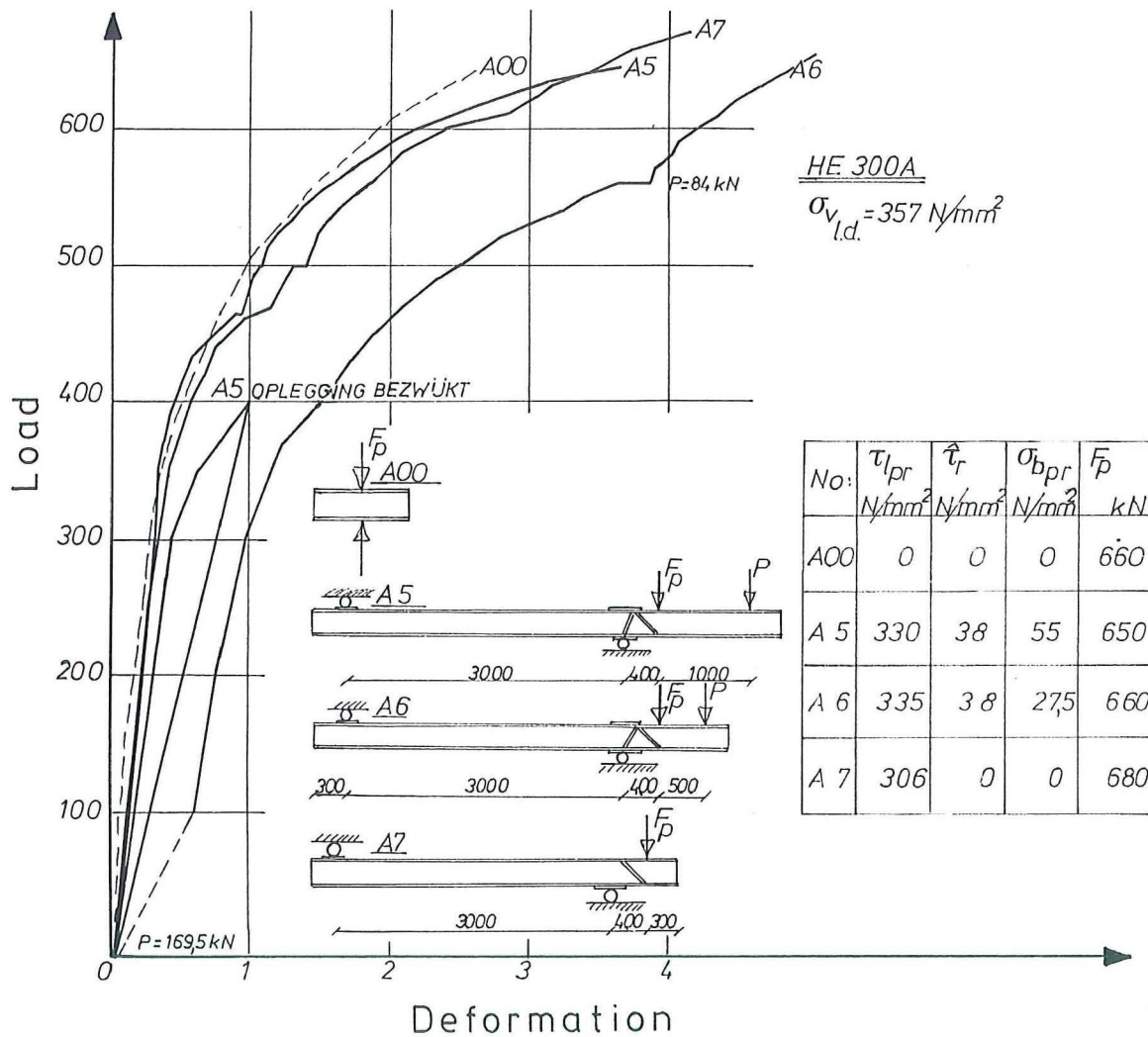
Figure. 3.3.3

(low or no shearing stress)



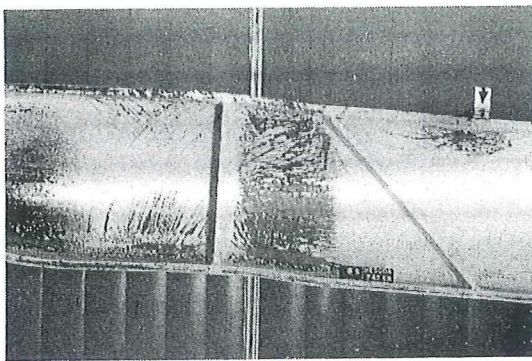
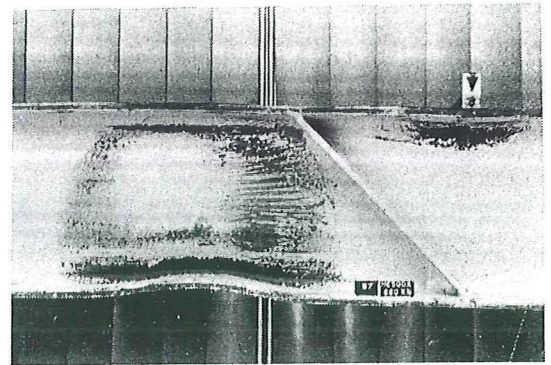
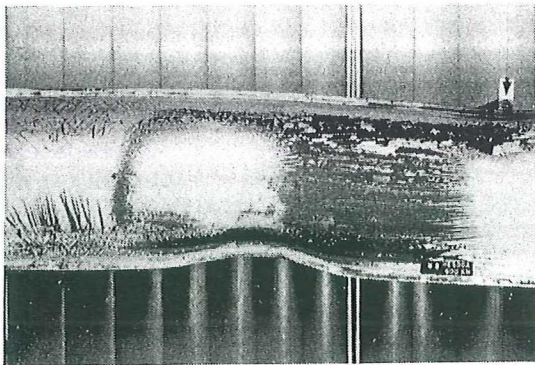
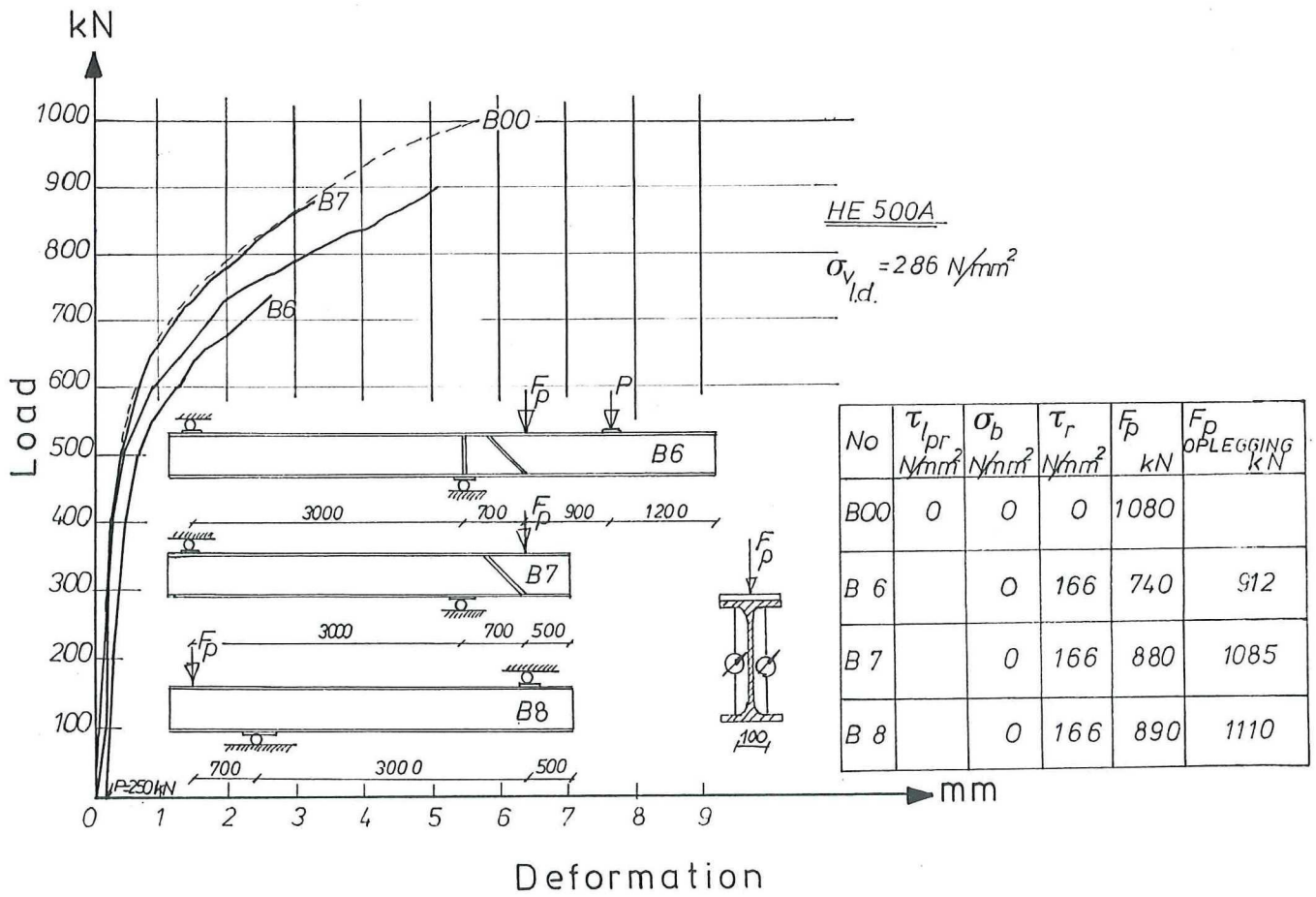
Influence of shearing stress already present in the section before loading.

Figure. 3.4.1



Influence of tensile stress caused by bending already present before loading.

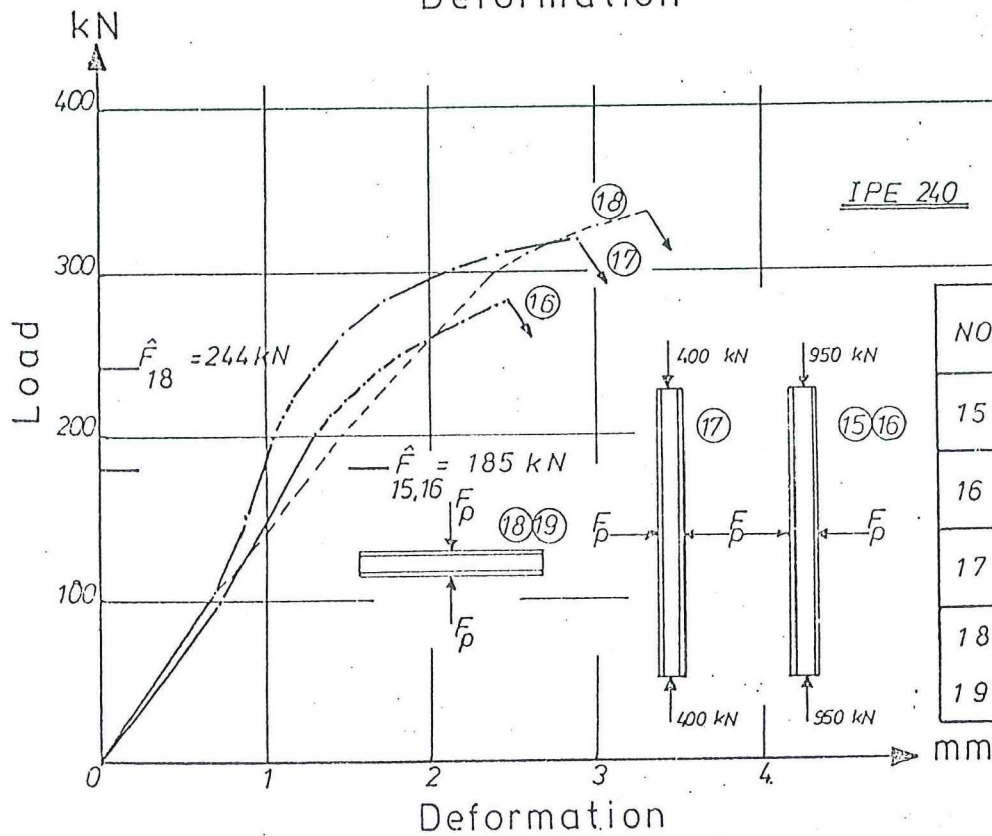
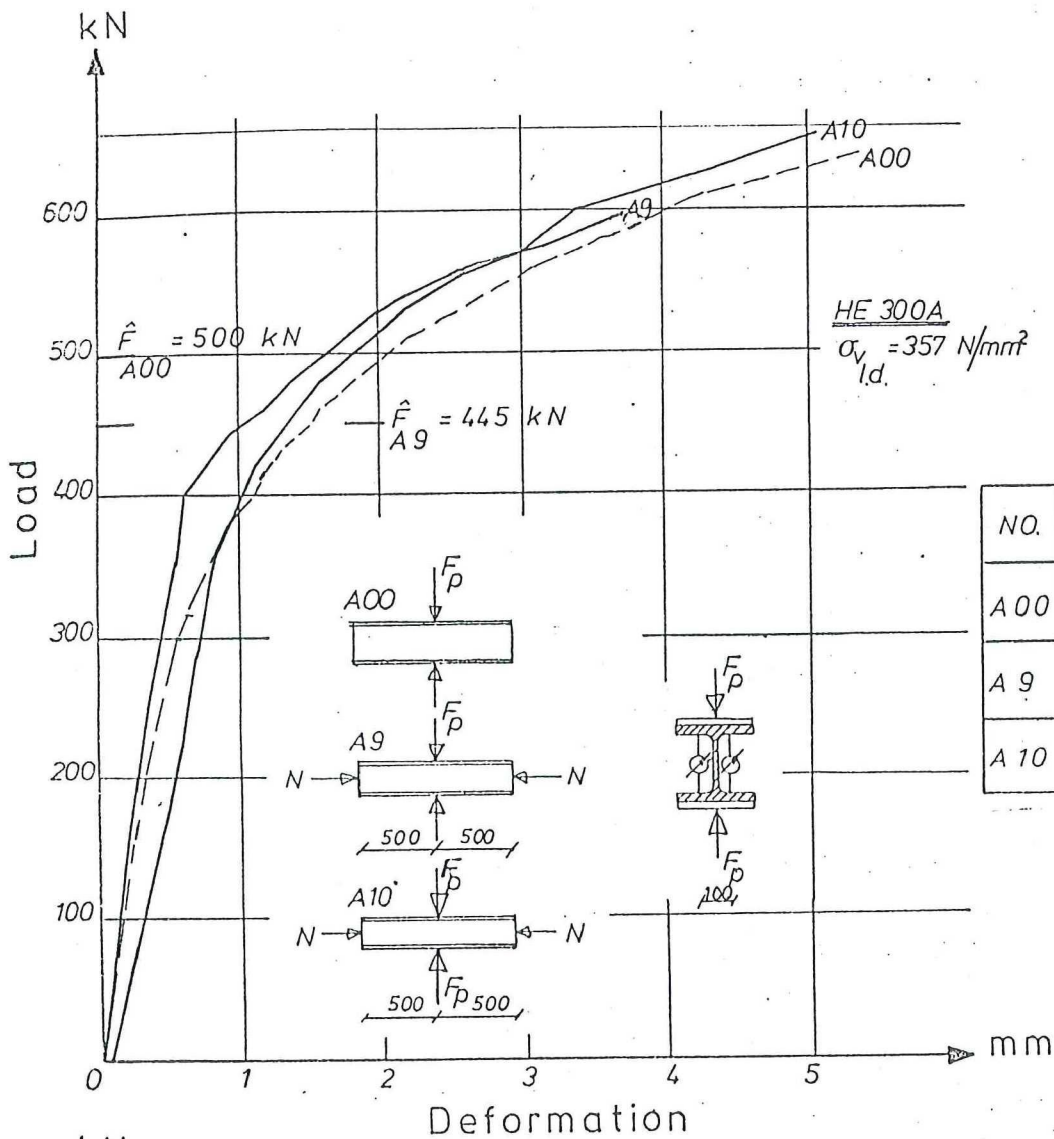
Figure. 3.5.1



Photographs of specimens after collapse.

Specimens collapsed over the support.

Figure. 3.6.1



Influence of compression force already present before

Figure. 3.7.1